UNIVERSITY OF GAZİANTEP

GRADUATE SCHOOL OF

NATURAL & APPLIED SCIENCES

THERMOLUMINESCENCE DOSIMETRIC PROPERTIES OF

$Ba_2SiO_4:Dy^{3+}$ SYNTHESIZED BY HYDROTHERMAL METHOD

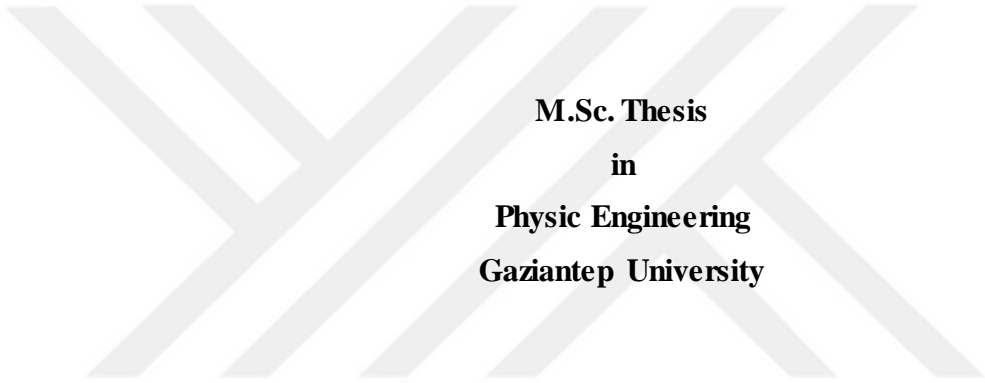### M. Sc. THESIS

IN

ENGINEERING PHYSICS

BY

AWARA ALI OTHMAN

DECEMBER 2017

Thermoluminescence Dosimetric Properties of $Ba_2SiO_4:Dy^{3+}$ Synthesized by Hydrothermal Method

M.Sc. Thesis

in

Physic Engineering

Gaziantep University

Supervisor

Assoc. Prof. Dr. Vural E. KAFADAR

by

Awara Ali OTHMAN

December 2017

REPUBLIC OF TURKEY
UNIVERSITY OF GAZİANTEP
GRADUATE SCHOOL OF NATURAL & APPLIED SCIENCES
PHYSIC ENGINEERING DEPARTMENT

Name of the thesis: Thermoluminescence Dosimetric Properties of Ba_2SiO_4: Dy^{3+} Synthesized by Hydrothermal Method
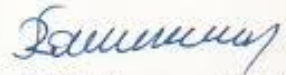
Name of the student: AWARA ALI OTHMAN

Exam date: 05.12.2017

Approval of the Graduate School of Natural and Applied Sciences

Prof. Dr. A. Necmeddin YAZICI

Director

I certify that this thesis satisfies all the requirements as a thesis for the degree of Master of Science.

Prof. Dr. Ramazan KOÇ

Head of Department

This is to certify that we have read this thesis and that in our consensus opinion it is fully adequate, in scope and quality, as a thesis for the degree of Master of Science.

Assoc. Prof. Dr. Vural E. KAFADAR

Supervisor

Examining Committee Members:	Signature
Prof. Dr. A. Necmeddin YAZICI	
Assoc. Prof. Dr. Vural E. KAFADAR	
Assist. Prof. Dr. Tuba DENKÇEKEN	

I hereby declare that all information in this document has been obtained and presented in accordance with academic rules and ethical conduct. I also declare that, as required by these rules and conduct, I have fully cited and referenced all material and results that are not original to this work.

Awara Ali OTHMAN

ABSTRACT

THERMOLUMINESCENCE DOSIMETRIC PROPERTIES OF $Ba_2SiO_4{:}Dy^{3+}$ SYNTHESIZED BY HYDROTHERMAL METHOD

OTHMAN, Awara Ali
M.Sc. in Physic Engineering
Supervisor: Assoc. Prof. Dr. Vural E. KAFADAR
December 2017, 59 pages

In the present work, %3 Dy^{3+} doped barium silicates $Ba_2SiO_4{:}Dy^{3+}$ prepared by hydrothermal method and the Thermoluminescence (TL) properties were investigated in detail. The crystal structure of $Ba_2SiO_4{:}Dy^{3+}$ was determined to be orthorhombic crystal system with Pmmm space group (PDF: 01-077-0150). TL glow curves of $Ba_2SiO_4{:}Dy^{3+}$ was recorded from 1 min to 8-hours exposure by beta source ^{90}Sr- ^{90}Y ($\approx$ 0.04 Gy/s). The Additive Dose (AD), Variable Heating rate (VHR), Peak Shape (PS), and Computerized Glow Deconvolution (CGCD) methods were used to determine the kinetic parameters namely the order of kinetics (b), activation energy (E_a) and the frequency factor (*s*) associated with the dosimetric Thermoluminescent (TL) glow peaks of $Ba_2SiO_4{:}Dy^{3+}$. The results of the experiments showed that $Ba_2SiO_4{:}Dy^{3+}$ composed of five general order TL glow peaks. The fading characteristics of the samples were also studied over a period time. The samples were irradiated and stored in a darkroom at room temperature. At the end of the planned storage times, the normalized TL area of $Ba_2SiO_4{:}Dy^{3+}$ reduced 60% of its original value. To eliminate this problem, we suggest adding several co-dopants into host lattice. Hence, our measurements provide some additional information about properties of $Ba_2SiO_4{:}Dy^{3+}$.

Keywords: Thermoluminescence, $Ba_2SiO_4{:}Dy^{3+}$

ÖZET

HİDROTERMAL YÖNTEMLE SENTEZLENEN Ba_2SiO_4:Dy^{3+}'IN TERMOLÜMİNESANS DOZİMETRİK ÖZELLİKLERİ

OTHMAN, Awara Ali
Yüksek Lisans Tezi, Fizik Mühendisliği
Danışman: Assoc. Prof. Dr. Vural E. KAFADAR
Aralık 2017, 59 sayfa

Bu çalışmada, %3 Dy^{3+} katkılı baryum silikat (Ba_2SiO_4:Dy^{3+}) hidrotermal yöntemle hazırlanmış ve termoluminesans (TL) özellikleri ayrıntılı olarak incelenmiştir. Ba_2SiO_4:Dy^{3+} 'ün kristal yapısı**,** Pmmm uzay grubuna sahip ortorombik kristal sistemi olduğu tespit edilmiştir. (PDF: 01-077-0150). Ba_2SiO_4:Dy^{3+} örnekleri ^{90}Sr- ^{90}Y ($\approx$ 0.04 Gy/s) beta kaynağı ile 1 dakika ila 8 saat arasında ışınlanmış ve ışıma eğrileri elde edilmiştir. Kinetik parametreler; kinetik derece (b), aktivasyon enerjisi (Ea) ve frekans faktörü (s) 'nün belirlenmesi için değişken doz, farklı ısıtma hızları, tepe şekli, üç nokta ve bilgisayarlı ışıma eğrisi ayrıştırma yöntemleri kullanılmıştır. Deneylerin sonuçları, Ba_2SiO_4:Dy^{3+} 'ün genel dereceye sahip beş ışıma tepesinden oluştuğunu göstermiştir. Numunelerin sönümleme özellikleri de farklı zaman aralıklarında incelenmiştir. Planlanan depolama sürelerinin sonunda, Ba_2SiO_4:Dy^{3+} 'ün normalize edilmiş TL alanı orijinal değerinden 60% oranında azalmıştır.

Anahtar Kelimeler: Termolüminesans, Ba_2SiO_4:Dy^{3+}

To My Parents

ACKNOWLEDGEMENT

TABLE OF CONTENTS

Page

LIST OF FIGURES

LIST OF TABLES

LIST OF SYMBOLS/ABBREVIATIONS

TL   Thermoluminescence

PL   Photoluminescence

C.B   Conduction Band

V.B   Valence Band

b   Kinetic Order

S   Frequency Factor

E_a Activation Energy

K   Boltzmann Constant

OTOR   One Trap One Recombination

β Heating Rate

μ_g Geometry Factor

CGCD   Computer Glow Curve Deconvolution

AD   Additive Dose

LLP   Long Last Phosphorescence

CHAPTER 1

INTRODUCTION

1.1 General

From the beginning of the world to today, people and other living beings lived under the influence of radiation. Radioactive materials and cosmic rays are the sources and reasons for the existence of this radiation in the world. It can be defined radioactive material by the substance that naturally emitted light, uranium, potassium, and thorium, are some examples of radioactive materials. These materials embrace ray as an example of gamma, alpha, and beta which are often a destructive creature. As already mentioned, our environment and climate are exposed to constant radiation. The measurement and study of this radiation have become valuable for scientific studies, mainly for those on the health of living creatures. A device used for measuring (exposure, absorbed dose, kerma, equivalent dose) or other related quantity called dosimeter. In the current scientific world after too much searching and hard work discovery of ionizing radiation, it was pretty benefit and suitable for many fields like science, technology, medicine, engineering, and etc…, the exact amount of radiation energy absorption in the exposed material in all application are an important factor to get the desired result. The best use can be achieved mostly by accurately determined the energy absorbed by the radiation field, inside the material it is possible to be distributed this energy is absorbed. These quantities measure the basis of measurement of radiation doses, referred to as the systems used for this purpose dosimeter. Dose measured by the unit of gray (Gy) or sievert (Sv). The new definition of gray in the (SI) unit is 1(joule) of radiation energy per 1(Kg) also equal (100) rad.

Advanced technology workers have worked for estimating dose radiation and for this purpose they are studying, organizing and investigating many analytical methods. These are some important technics are preferred, (Loyoluminescence technique, Fluorescence technique, Diffused Reflectance technique, Optically Stimulated Luminescence technique (OSL), thermally stimulated luminescence technique (TLD),

Electron Paramagnetic Resonance technique (EPR dosimetry)). The radiation dose received by phosphorus and TL output is directly proportional to each other this is the main basis in thermoluminescence, therefore supply the wherewithal of estimating unknown radiation. The treatment of light (TL) is used as a non-negative measure, that the level of radiation over a long period of time, that is useful for monitoring radiation and continued with field staff (radiologists) integrated control. Weekly dose month of the year, according to the number of permits. In any case, it should be recognized that the majority of phosphorus TL in structural equivalent (in terms of energy absorption under irradiation), that is related to the dose, from the viewpoint of protection, and the radioactive factor is not easy. LiF, LiF: Mg, Ti (TLD-100), LiF: Mg, Cu, P $Li_2B_4O_7$: Mn, according to the equivalence of the TLD, TLD material widely used in medical applications. Through the organization of the use of the TLD material in medical applications such as high-sensitivity as $CaSO_4$: Dy, Al_2O_3, and CaF_2: Mn, used.

TL dosimeter is a very high potential application and TL very helpful in many fields due to their favorable properties. Favorable properties of TL such as high sensitivity, recyclability, environment-insensitive terms, and conditions, small in size, possible point dose measurement, many TLDs can be exposed in a single exposure, existing in various form (powder, ribbon, chips and rods…), not expensive, reasonably equivalent tissue [15]. In the earlier, professionals had experienced the technique of film budge in practice, and then they found that the technology of TLD is better for many reasons. While the last 3 for 4 decades, they have developed and established the TLD technology. This became popular prominent applications of dosimetry and radiation thermoluminescence protection. Daniel et al, for the first time, used the thermoluminescence phenomenon for the dosimetric purpose [1]. Wide-scale dosimetry devices for phantom applications and in vivo medical applications are dose measurements. Another field where the TL dosimeter is realized personal monitoring (Personal Surveillance) radio-therapists. Micro-Gray is widely used in dosages due to long-term exposure to low integration to reduce environmental monitoring systems. TLDs have been used in monitoring measures such as leakage radiation on and around source containers, air dispersion measurement around open facilities, monitoring of the area around radiation facilities, etc. The rapid fade ratio of the main TL temperature at a low temperature of certain phosphors such as $CaSO_4$: Dy was used for the estimation of the exposure time after irradiation.

It has been demonstrated that this technique also makes it possible to detect and evaluate the thermal and fast neutrons doses. Since TL phosphors are insensitive to thermal neutrons, a combination of them can be used to measure the dose to estimate the dose of thermal and gamma neutrons in a mixture field.

In addition, the thermoluminescence dosimeter enters the archaeological dating, ancient ceramic and ceramic dating, and for some reason its suitable and successful method, firstly the exact date of the sample (kiln) can be taken other method heavily depend on form and style of the pottery, which is civilized, secondly TL dating method until 30,000 years later, age restriction is 50 years old with an accuracy of $\pm$ 1 year, also with this method, counterfeit authentication and detection can be done quickly and easily [4]. It can simply be calculated by dividing the cumulative dose by the annual dose and can find an archaeological age, but in fact, there are many complex factors in the way to assess age. Areas of radiation and non-radiative radiation measuring devices such as ultraviolet light, and ultrasonic dosimeters. By applying the amount of UV consciousness of the thermal response of the human skin it is possible to measure the value of UV energy effectively.

Thermoluminescence also used in the application of agriculture. In this regard, TL used in particular with a high level of photon dose measurements as a measure of protection in the case of the concept of food, radiation of seed, pest control and so on. Officially, dose measurement in agriculture focusing on the victims of chemical dosages, for example, ferric for $(Fe_2{}^+, Fe_3{}^+)$ system. The construction of TLDs has been applied a less expensive method, in range (10^{-4}) to (10^{-8}) rad [3]. As we mentioned before it could be seen the application of TLD in many areas of life so can be seen in a field of biochemical and biological application, inevitably all measurements are in range LNT-RT, efforts successful in the study of hydroxyl and amino benzoic acid acids, proteins, nucleic acids, plant leaves, algae, and bacteria. The TL results may indicate accurate stability of ortho or benzoic acid forms (inter and intro) molecular transitions of radioactivity in proteins and nucleic acids, these components may be associated with TL behavior. The optical transmission method can be linked to TL and an additional path set Z graph, and from the TL pattern, the interaction between salt and protein can be understood [8].

TL used in forensic science and criminological science, the actual examination of criminological sciences is to develop and institutionalize techniques to look at the evidence with comparable materials known the starting point, which is constantly available at the moment amounts and is required to be broke down nondestructively for confirmation purposes. Thermoluminescence can offer an appealing system chose materials that regularly experience in criminal cases namely; glass, earth, safe material protection and so on. This can be utilized as an exclusion prove that at the point when the TL qualities not coordinate it can be said with certainty that a particular sample does not originate from a known source. To reduce the likelihood of accidental consolidating and increasing the certainty of the TL estimates whose flag to call out portion can be terrible, maybe control performed by the TL glow curve from virgin samples and also for a substantial simulated gamma or x-ray light and also the discharge spectra [3].

TL from the earliest also used in the field of geology, TL from the most punctual likewise utilized as a part of the field of topography for a different reason, for example, sedimentation, igneous activities, the dating of mineralization and assessment of development rate of shorelines and sand ridges. At present utilizing single grain system time of topographical examples can be evaluated up to 50 million years with a precision of +5% or −5% [3].

Thermoluminescence in 1938 was used in ceramic products to control feldspar where some quantitative studies are unchanged, by the levels of imitation it can determine the distribution of a TL that give a close to the manufactured light by a special feldspar. The ceramic industry is similar that the exceptional technique is to repeat that multiple occasions to spare packs of a few materials, and your formations of controlled substances, feldspar can be controlled quickly and viability.

It is clear that in the world it can't obtain 100 percent of pure material, this means that every material has impurity so study and understanding of defect in a crystal or solid material, it is very important first to understanding and finding the properties of this material and secondly knowing of characteristics of material help the scientist and other researchers to understand some phenomena and to find the best material for the sensible application so TL is one of the techniques that use for this purpose. By the effect the disfigurement or defect in a material structure as we mentioned before the

physical properties of solid it can be determined. A fundamental noteworthiness about the imperfect structure is essential for the depiction of the material and in like a way for the impression of various physical properties. By a few unmistakable systems, for instance (warm, electrical, optical extra), the imperfection structure of a material ought to be considered. Thermoluminescence is the spread of light or is the phenomena that happen when non-metal material like (insulator and semiconductor) prior assimilation of vitality from radiation and then after warming the substance emit these stored energies in form of light [1,2]. According to a photomultiplier tube circuit can be measured the light that spread from the non-metal material as a component of temperature it is named glow curve. The TL dosimeter glow curve in 1945 determined by Randall and Wilkins for the first time. The first peaks discovered in glow curve is multiple peaks and then reported the rare of the occurrence of single peak [5]. It can get a valuable information from the glow curve about the activation energy (energy level of the situated trap), the number of recombination of the (electron-hole) pair also can be determined in the crystal by display area under the curve. The factors like, types of dopant, the level of radiation dose, defect center after irradiation, host or mixture of radiation compound, type of ionizing radiation and annealing are affected the final glow curve structure [6,7].

1.2   Historical Background

Phenomena of luminescent have charming and engrossing humanity inasmuch the earliest time Bolognian Stone (BaS) described as the luminescent material for the first time. An Italian Alchemist, Vincenzo Cascariolo depict the first artificial phosphor in European literature dates around 1603, that used natural mineral barite in an attempt to create gold, but he obviously did not obtain gold instead he observed a persistent luminescent material after heating the stone under reduction condition. He named this rock Bolognian stone because he founded near Bologna, which became famous and a topic of study and appreciation and approval for decades. Thus the first synthesized sulfide phosphor is (BaS). Bolognian stone was given several names until the modern name for all luminescent material (liquid or solid) become ''PHOSPHOR'' [9]. But German physicist Eilhardt Weidman, in 1888 used luminescence word for the first time. From seventeenth-century thermoluminescence studies start as a limb of luminescence.

Empirical observation of thermoluminescence phenomena of the mineral is around 1663 by Robert Boyle, he noticed the glowed off the diamond when held near a hot but non-luminous piece of iron [14]. However, diamonds are not the only material, the other metals like quartz flint feldspar and calcite are release light when they are warming [7]. As well, these scholars Johann Sigismund Elsholtz and Henry Oldenburg manage the experiments to see the radiation of mineral due to warming.

The phosphorus as a green stone powder was observed by George Kaspar Kirchmaier and he blended with water and after heating, it gleamed [13]. In the eighteenth century, Dufay indicated to lighting as a kind of burning. As well he found that the material loss of the thermoluminescence if pretty much heating after he worked on many elements (mainly chlorophane). The prior acknowledged stones are categorized into three kinds due to a luminescence by heating (1) stones have within a Hepar (Fois) or Sulphur, Sulphur compound burned in the free air. (2) Those after they received light emit it, for example, a diamond. (3) Those under hot water luminescence which do not require air like fluorspar and dolomite [13]. Nevertheless, till the end of the 19th century, it was not understood that the energy applied externally and accumulated in the substance until it was issued through the application of adequate thermal energy, but in 1894 Dewar for the first time gave information about this. Dewar experimented on calcium sulfide which was irradiated and at 90°K on heating, he noticed the light, this test provided a general method for studying thermoluminescence in crystals that are as yet used. After that Dufay's study carried to the new level by Canton. When Canton raising the temperature of phosphorus he finding a new type of light, which he referred to as the thermoluminescence of the unnatural phosphorus [13]. He declares that fluorescence intensity is a level display of thermoluminescence. The latter conducted a study on the thermoluminescence and the luminescence that reflects the illumination (triboluminescence) is the result of friction. Here he finds that he cannot find a solid relationship between two types of luminescence. In the nineteenth century, scholarly and studies continued on thermoluminescence. Heinrich is one of the researchers referred that almost all elements in the form of powder have the ability to emit light when subjected reasonable heating. Theodor Von Grotthus is the researcher coincide and agree especially with a fluorspar, and showed the community between of thermoluminescence substance and essence in the emitting light, both are made of the positive and negative part. Later opposing Grothus David Brewster is one of the world

claims that he cannot always restore the luminescence property to expose the minerals to light.

1.3 Luminescence

Semiconductor and insulator are nonmetal substances also it could say that its stable materials that absorb radiation energy from the exposure radiation and gathered exceed energy this is causing the material be unstable, due to behavior of material that wants to be stable release this gathered energy as light the process named "luminescence" if light emitted by longer wavelength (Stokes' law). The wavelength of the emitted light is not represented by the incident radiation, so characteristic of luminescence substances could be achieved and recognized from the emitted light. Visible light is not only range from electromagnetic spectrum that spread or emitted from the substance, other wavelength range (ultraviolet or infrared) from the electromagnetic wave can be spread [2].

Luminescence can be classified according to the parameter (τ_c) called characteristic or delay time as shown in Figure 1.1.
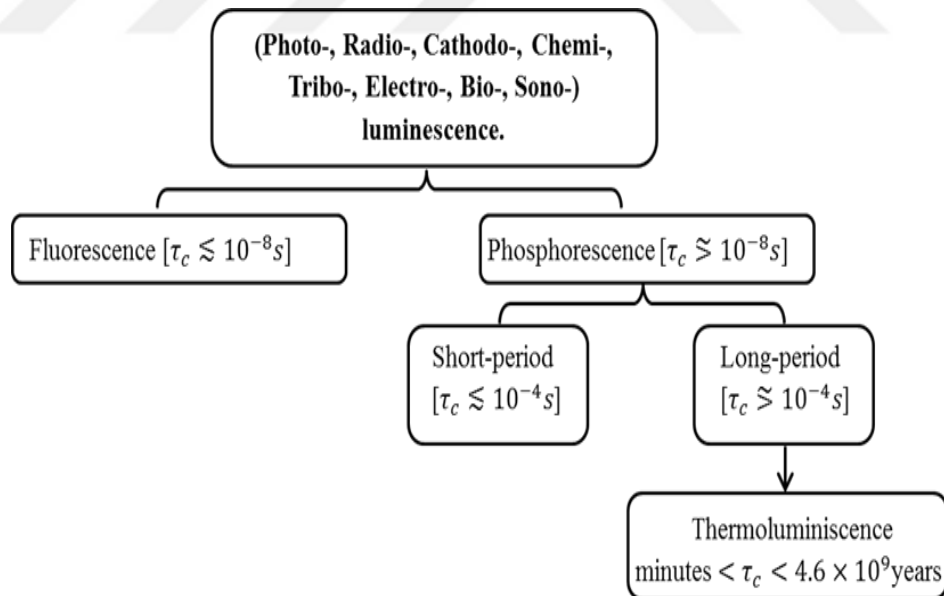
Figure 1.1 The family tree of the phenomenon of luminescence [12].

Characteristic time is the time needed to take place of phenomena light emission. Fluorescence directly or need a little time to happen (τ_c less than 10^{-8} sec) and immediately ended by cutting or turning off the radiation source, but phosphorescence

need more time to happen (τ_c greater than 10^{-8} sec), and for a period of time, it will be continued after turning off or cutting radiation source. Phosphorescence also subdivided into two parts due to the continuity of phenomena after removing the source of radiation first called short period and the range of characteristic time (τ_c) between (10^{-8} to 10^{-4} sec) and the second one is a long period which $\tau_c \geq 10^{-4}$. So it's clear that in fluorescence there is not metastable state (trapping state) for an electron in the energy gap, electron immediately in the excited state come back to the ground state after cutting radiation means that temperature independent.

But in phosphorescence electron are trapped in the metastable state this means that electron immediately and easily doesn't go back to the ground state need extra energy to release in the trap, after electron gain enough energy can leave trap to excited state after that come back to the ground state. If the applied energy is in the form of heat phenomena called thermoluminescence its one of the type of phosphorescence, phosphorescence is temperature depended. The existing state in the crystal lattice generally described by energy band theory. So light emission can be explained by the transferring energy to the electron from the energy radiation, and electron leave ground state (g) after gain enough energy go to the excited state (e) shown in figure 1.2a (transition i), and photoluminescence emitted due to come down electrons from excited state to ground state (transition ii).

The process called fluorescence if the average time less than (10^{-8} sec) between excitation and lifetime of emission which is described in figure (1.2a) also its independent of temperature. But sometimes electron trapped by the metastable state which is situated between the ground state (g) and excited state (e), and in this state, the electron may stay until gain extra energy to go to the excited state (e) and release extra energy in the form of light when coming down to ground state (g) naturally. Thus trapping center caused the electron to delay (second for years) or caused the delay between the process of excitation and process of light emission. The remaining and spending the time of electron in the trap as a function of circumfused temperature given:

$$\tau = s^{-1} \exp(E/kT) \tag{1.1}$$

Frequency factor (s) is constant, and k is Boltzmann's constant, E is trap depth (the difference of energy between two state trap and excited state).

Thus phosphorescence is exponentially temperature dependence [2]. As it describes above, a temperature is most different between phosphorescence and fluorescence.
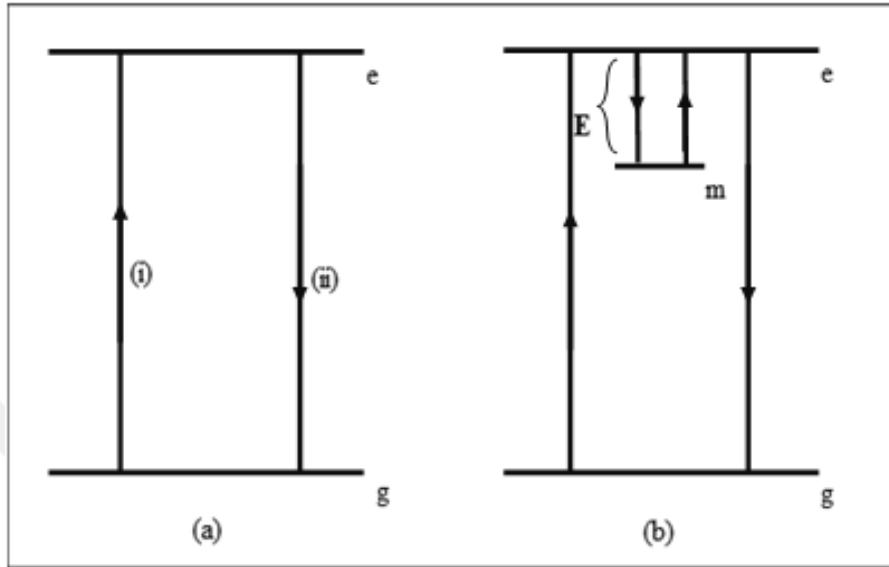
Figure 1.2 The energy level diagram of (a) fluorescence, and (b) phosphorescence production [12].

According to the method of excitation type of luminescence can be classified for many types, as it is seen in Table 1.1.

1.4   Thermoluminescence

The substance like semiconductor and insulator are emitted light by heating them but when before they have stored energy from the exposed radiation this phenomenon that thermally stimulated called thermoluminescence. Anyway, this simple explanation does not describe the exact thermoluminescence mechanism [9,16].

The light emitting from thermoluminescence process is different from spontaneously emitted light from incandescence (light from heat energy). From the incandescence case things (materials) it will shine whether at high enough temperature warming. When the warm metal of the fireplace is placed in the fire it starts to shine "red heat", which is incandescence. It is amazingly "hot white" by the same means, just like when standard bright vibrant tungsten fibers were warmed more violently by flowing

9

current. The shining of sun and stars also because of burning (incandescence). The emission light in thermoluminescence is stimulated thermally so in this case among the forbidding gap (energy gap) some energy level it needs to add, for the material host lattice by inserting some impurities in the forbidding gap the level of energy in the gap created. The state named the metastable state in thermoluminescence material. Lattice defects naturally or unwittingly occur and in the band gap induce electronic state. Although to understand phenomena of thermoluminescence lattice defect it's an important parameter that used [10,11].

Three fundamental factor in thermoluminescence production necessary. Firstly semi-conductor and insulator according to their structure are only materials used metal doesn't use for thermoluminescence production. Secondly, it must heat the material to triggered light emission. Finally, the material must gain and stored energy by absorbing energy from the radiation exposure. In thermoluminescence after the stored energy emitted in the form of light by heating, the material after cooling once more must store energy by irradiated it to again emitted light by warming because the material is not capable by simply cooling the pattern and re-heating one more time release thermoluminescence.

Table 1.1 The category of luminescence and excitation method [8].

luminescence phenomena	Methods of Excitation
Bioluminescence	Biochemical reactions
Cathodoluminescence	Electron beam
Chemiluminescence	Chemical reactions
Electroluminescence	Application of an electric field
Photoluminescence	U.V. and infrared light
Piezoluminescence	Pressure (10 $tons/m^2$)
Triboluminescence	Mechanical, Frictional forces
Radioluminescence	Ionizing radiation
Sonoluminescence	Sound waves
Fluorescence	Ionizing radiation, U.V. and visible
Phosphorescence light	Ionizing radiation, U.V. and visible
Thermoluminescence	Ionizing radiation, U.V. and visible
Lyoluminescence	Ionizing radiation, U.V. and visible

1.5   Layout of Thesis

This thesis consists of 6 chapters arranged following:

• Chapter 1 introduces the context and contains historical subject matter, and the other two sections devoted to a description of luminescence and thermoluminescence.

• Chapter 2 is describing the results of other researcher and what they founded in their result.

• Chapter 3 separated into two sections first, Thermoluminescence Models which described in detail. Second, involved three methods to find out Trap Parameters.

• Chapter 4 includes the material synthesis and doping procedures, Equipment's, Radiation Source with a brief characterize of Irradiation Procedure.

• Chapter 5 presents the results of the study of the experiments stated in Chapter 4 with some determination of trap parameters. These results include the outputs from characterization analysis as well as thermoluminescence measurements.

• Chapter 6 discusses the main findings of this study and recommendations.

CHAPTER 2

LITERATURE REVIEW

Many researchers used barium silicate as the host material in thermoluminescence studies and they used different methods to achieve the various form of it.

Yamaga et al and another co-worker in 2005 studies barium silicate (Ba_2SiO_4) and (Ba_3SiO_5) that was doped by Eu^{2+}, barium silicate next radiated with UV light and the broadband luminescence of (Ba_2SiO_4) and (Ba_3SiO_5) produced with peak wavelength of 510 and 590 nm respectively. The intensity of long-lasting phosphorescence was measured as a function of temperature and time. The decay time radiation in the wide range of $1-10^3$ sec was distributed beside the fluorescence lifetime of Eu^{2+} ($\sim 10^{-6}$ sec). After one second the decay curves were fitted (t^{-n}) where $(0.2 < n < 3)$ in the temperature range of 100-500K. The long-lasting phosphorescence temperature dependency in a time domain integrated follows the Arrhenius equation which was modified by the use of thermal activation energy including the process of radiation and non-radiation decay. Finally, they reported that by UV excitation the produced electrons and holes in the crystal through thermal hopping and tunneling moved back to Eu^{2+} sites and at Eu^{2+} recombine radiatively [17].

Yao et al and colleagues in 2009 are studied the photoluminescence property of $Ba_2ZnSi_2O_7:Eu^{2+},Re^{3+}$ (Re=Dy, Nd) by using the combustion-assisted synthesis (CAS) method. The alkaline earth silicates were prepared in the forms of $Ba_2ZnSi_2O_7:(Eu,Dy)$, $Ba_2ZnSi_2O_7:(Eu,Nd)$ and $Ba_2ZnSSi_2O_7:(Eu, Dy, Nd)$. The obtained phosphors were characterized by means of X-Ray Diffraction (XRD) and their Photoluminescence Spectrum (PSL). A single band that centered at 503 nm can be observed in the emission spectrum, which corresponds to the $4f^65d^1 \rightarrow 4f^7$ transition Of Eu^{2+} when the $Ba_2ZnSi_2O_7:Eu$ phosphors doped by Dy^{3+} and Nd^{3+} ions, then the blue-green afterglow $\lambda_{em} = 503nm$ can be observed. Also for Eu^{2+} in $[EuO_8]$ the value of electron affinity (ea) was calculated and is equal (1.63eV).

Also, the afterglow of the phosphors is enhanced when $(Dy^{3+}$ and $Nd^{3+})$ quenching concentration was over 0.07 [18].

Meiyuan Wang, Xia Zhang and other in 2010 the enhanced blush green LLP phosphorescent of N contained $Ba_2SiO_4 : Eu^{2+}$ for x-ray and cathode ray tubes are reported and by using the conventional high-temperature solid-state method with the chemical formula $Ba_2SiO_4 : 0.01\,Eu^{2+} - xSi_3N_4 - 2BaCO_3$ (x=0.1 to 1.0) under weak reductive atmosphere were prepared. As a function of Si_3N_4 content the TL and LLP phosphors properties have been investigated next exposure of X-ray. With increasing the content of Si_3N_4, the phosphorescence grows super-linearly and some new TL peaks appear at low temperatures of about 400, 355, 365, and 335 K. These peaks are attributed to the formation of new traps related to the N substitution for O. The high content of High Si_3N_4 can promote two or more traps to form a complex trap to improve the ambient temperature LLP. The temperature dependence of the PL intensity reveals that the thermal stability of the phosphors for the relatively high content of Si_3N_4 is better than that of the low content of Si_3N_4 [19].

Tatsuya Sakamoto and colleagues in 2011 were reported about single crystal growth of $Ba_2SiO_4 : Eu^{2+}$ that was succeeded by a novel synthesis method in which gas (SiO) and solid $(Ba - Sc - Al - Eu - O)$ phase were hybridized. The $Ba_2SiO_4 : Eu^{2+}$ mono-crystal was synthesized at $1600\ ℃$ by crystal growth of the interface after reaction the SiO gas on the surface of the $(Ba - Sc - Al - Eu - O)$ substrate in a reducing atmosphere and had plate shape with size of $500\ \mu m$ and the monocrystal under 300-450 nm excitation emitted green light around 500 nm, which exactly agree with the spectrum of the $Ba_2SiO_4 : Eu^{2+}$ powder in the conventional solid-state reaction [20].

Huayna Cerqueira Streit and other in 2013 were studied the red, green, and blue photoluminescence of $Ba_2SiO_4 : M$ $(M = Eu^{3+}, Eu^{2+}, Sr^{2+})$. Energy and time-saving combustion synthesis were applied flexibly to the preparation of doped and un-doped barium orthosilicate nanoparticles resulting in very small nanoparticles with a size of about 35 nm. Different approaches were used to obtain red-green-blue emission and Ba_2SiO_4 NPs was doped with Eu^{3+}, Eu^{2+} and Sr^{2+}, respectively. Substitution of Ba^{2+} ions with Sr^{2+} ions leads to lattice defects, which are stabilized by in situ lattice imperfections of Ba_2SiO_4 nanocrystals. In this way, it was possible to generate blue emission of Ba_2SiO_4 nanoparticles free from rare earth for the first time. In addition,

the properties of the luminescence defects on $Ba_2SiO_4 : Sr^{2+}$ NPs have been studied using temperature spectroscopy of UV/VIS and measurement of the lifetime. This is due to the presence of impurities-trapped excites, trapped at the Sr^{2+}, causing distortion in the lattice then stabilizing excite. At temperatures above $T_q = 120$-$130\,K$, the blue emission is quenched efficiently, but suddenly an orange emission occurs at $16,643\,cm^{-1}(600\,nm)$. A model explaining this atypical behavior, which is consistent with the temperature dependence and similarity of the observed emission decay curve and the excitation spectrum, is suggested. In the lattice, it involves the thermally activated movement of impurities trapped excitants into another Sr^{2+} site, which implies non-radiative relaxation and leading to a redshift of emission. However, photoconductivity and thermoluminescence measurements will help to clarify the participation of conduction band in the proposed mechanism. Additionally, the Scherer equation was combined with SEM and AFM images to characterize the particle size. Finally, it has been demonstrated that a stable suspension can be made in a liquid medium that emits green light when the generated $Ba_2SiO_4 : Eu^{2+}$ NPs is irradiated with ultraviolet light [21].

J. I. Choi and co-worker in 2014 reported electrophoretic deposition of nano and micron-sized $Ba_2SiO_4 : Eu^{2+}$ phosphor particles. Electrophoretic deposition (EPD) is a technique of depositing charged particles from a stable suspension under the force of an applied electric field. Nanoparticles of various materials are covered by EPD, but direct comparison is hardly done includes EPD of nano and micron-sized particles of the same material. This study was done for the purpose of rapprochement the EPD of nano, nano-core/SiO_2 shell and micron-sized $[(Ba_{0.97}Eu_{0.03})_2 SiO_4]$ phosphor particles for application to near ultraviolet LED-based light sources are there. EPD from a bath with amyl alcohol is able to produce a uniform film for all particle sizes, while a homogeneous film was made of single micron-sized particles in a bath of isopropyl alcohol. A new equation for the prediction of the deposited mass was developed, taking into account the change in the concentration of particles in the bath both from deposition and from precipitation, which agrees well with the experimental values [22].

Peng Jiu Wang and other colleagues in 2015 reported the sunlight activated long-lasting luminescence from $Ba_5Si_8O_{21} : Eu^{2+}, Dy^{3+}$ Phosphor. Persistent phosphors of

visible light are commonly used as freestanding night vision and fluorescent labeling materials. From the influence of the structure of the six-membered ring plane in $Ba_4(Si_3O_8)_2$, a similar structure of $Ba_5Si_8O_{21}$ which can exhibit better phosphorescence characteristics is expected. In this paper, for the first time, a novel visible long-lasting luminescence phosphor of Eu^{2+}/Dy^{3+} co-doped $Ba_5Si_8O_{21}$ it was reported. The phosphor of $Ba_5Si_8O_{21}:Eu^{2+},Dy^{3+}$ can be efficiently activated by sunlight or even under severe weather conditions, mainly due to a wide spectrum of excitation (200-455 nm) and strongly reacts with the rays UV-A and violet-light in the solar spectrum. After activation, $Ba_5Si_8O_{21}:Eu^{2+},Dy^{3+}$ emits strong radiation at (380-680) nm and shows persistent phosphorescence over 16h. In addition $Ba_5Si_8O_{21}:Eu^{2+},Dy^{3+}$ shows excellent stable phosphorescence even in water and indicating that it can be charged effectively and repeatedly by natural sunlight in all kinds of outdoor environments. Furthermore, it shows excellent and stable phosphorus even in water, which shows that $Ba_5Si_8O_{21}:Eu^{2+},Dy^{3+}$ is a full-blown material that can be efficiently and repeatedly by day-light in a variety of environments Outdoor-air, can be charged. In addition, the mechanism of afterglow shows the behavior of quantum tunneling [23].

Bi Zhang and colleagues in 2017 was studied the enhancement of the stability of green-emitting $Ba_2SiO_4:Eu^{2+}$ phosphor by hydrophobic modification. In this paper, a simple and feasible surface modification method proposed that suppresses moisture-induced degradation of $Ba_2SiO_4:Eu^{2+}$ ($BSO:Eu^{2+}$), which very strong impacts on its reliability and limits its wide commercialization in WLED. A hydrophobic surface layer was formed on the surface of this phosphor by hydrolysis and polymerization of tetraethylorthosilicate (TEOS) and polydimethylsiloxane (PDMS). A hydrophobic surface layer was formed on the surface of this phosphor by hydrolysis and polymerization of tetraethylorthosilicate (TEOS) and polydimethylsiloxane (PDMS). The surface layer produced consisted of an amorphous silicon dioxide with a thickness of ~2 nm with the presence of -CH 3 groups on the surface. The modified phosphorus exhibited superior stability under high-pressure water vapor conditions at 150 °C [24].

CHAPTER 3

THEORY OF THERMOLUMINESCENCE IN SOLID

3.1   General

As it's clear that the process of thermoluminescence is relatively a complex process so firstly in this chapter a simple model was used to explained the process of thermoluminescence then some assumption that was used for solving the equation of General Equation for One Trapping (GOT), these assumption named first, second and general- order kinetic that described in detail in here. Also, the method that was used for determining trapping parameter was explained.

3.1.1   Simple Thermoluminescence Model

The band theory of solid material is a good theory for interprets of the thermolumin-escence properties that observed as it explained in chapter 1. Most electrons for ideal insulator or semiconductor at room temperature are populated in the Valence Band (V.B), and at the same time in the Conduction Band (C.B) there is not populated of the electron, but it can fill by an electron. These two band separated by the gap (E_g) also called forbidden energy band gap. There are a few luminescence materials however not all are sufficiently proficient for the feasible purpose. To improve iridescence productivity of the material it's important to include a component which is called activator (ie. Dy in Ba_2SiO_4) to the host lattice. The activator then goes about as trap center and luminescence center.

When the material doped by the activator several states of energy (activation energy) which assigned to a level or metastable state produced within the forbidden gap (E_g). This model named one trap and one recombination center so simply have two states in the Eg, one for trapping electron and (T) one for trapping hole (R). If (E) greater than several (KT), when k is Boltzmann constant, then trapped charge remains in the trap for a long period.

For an electron, trap E is measured in (eV) from the trap level (T) to the bottom of (C.B). For a hole, the trap is measured from the trap (R) to the top of the (V.B) it's shown in Figure 3.1.

The solid bombardment of the energy $(h\upsilon > E_g)$ cause to the ionization means the production of free charge, produce a hole in the valence band due to the transition of an electron to the conduction band from the valence band.

At the same time electron are exist in conduction band transition (a) shown in Figure 3.1.
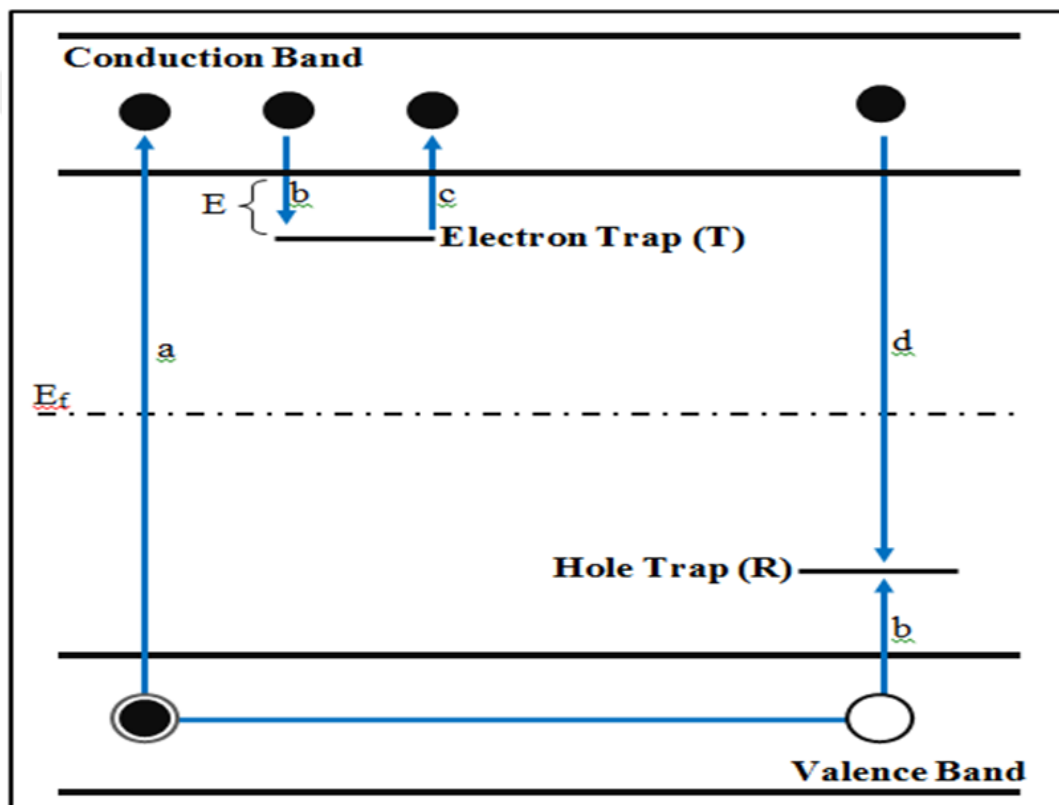
Figure 3.1 The model of the energy band for electronic transitions is given in a TL material according to the two-level model a simple (a) The occurrence of holes and electrons; (b) hole trapping and electron; (c) is the discharge of electrons because of thermal stimulation; (d) is recombination. (●) electrons, (o) holes, electron trapping level is T, the center of recombination is a level R and E_f is the Fermi level [25].

Next ionization process, there are two possibilities for the free charge carriers; firstly, the electron may be directly recombined with hole by a return to (V.B).

Secondly, electron and hole may be trapped by trap center (T) and (R) respectively shown in transition (b). Assuming that the excited solid previously is heated from the trap states electron charge can be released shown in transition (c) by supplied this energy (thermal energy).

According to the Arrhenius equation (equation 3.1) rate of energy can be measured that is thermal stimulation process or the releasing of electron probability can be described per time. It's clear to reach the equilibrium must be the energy barrier defeat and dominant.

$$p = s \exp(-E/KT) \tag{3.1}$$

From the Arrhenius equation the relation between T and E easily could observe, T is proportional change with E. In fact in the case $E \gg KT$, temperature with E always linear increase, with the Randall-Wilkin model this behavior agree, from the deeper trap the electrons need more energy and of course need higher temperature [26, 27]. After releasing electron then by indirectly transition (d) recombine with a hole (R) center by emitting light the process which is called thermoluminescence. Addirovich at 1956, in general case, to explain the phosphorescence decay used three differential equations, and after that, during the trap emptying process, this model for explaining the flow of charge between the two band (localized and delocalized) band was used by Haering-Adams and Halperin-Barner in 1960 [60].

The intensity of the photon that detected during trap emptying process is given by

$$I = -\frac{dm}{dt} = A_m \, m \, n_c \tag{3.2}$$

The negative sign from the first part of equation (3.2) means that the intensity of emitting photon increased for a limit of time then decreased due to the decreasing number of the hole in recombination center according to recombination process.

From the second part, it also could say that there is a proportionality change between recombination rate with the number of free electrons n_c (cm^{-3}) and number of hole in recombination center m (cm^{-3}) since A_m is the probability of recombination $(cm^3 \, sec^{-1})$ and independent temperature (constant).

The variation of electron population in (T) explained by equation (3.3) and consideration of electron excitation to C.B and also possible re-trapping, so

$$\frac{dn}{dt} = -np + n_c(N - n)A_n \qquad (3.3)$$

N is concentration of electron trap, $A_n(\text{cm}^3\text{sec}^{-1})$ is constant and its probability of re-trapping. According to the charge neutrality, it could find the changing number of electron in C.B per unit time

$$\frac{dn_c}{dt} = \frac{dm}{dt} - \frac{dn}{dt} \qquad (3.4)$$

Also, could write as equation 3.5

$$\frac{dn_c}{dt} = np - n_c(N - n)A_n - n_c m A_m \qquad (3.5)$$

This equation says that rate of free electron concentration in C.B is given by the rate of r = electron release thermally from (N) minus rate of re-trapping and recombination in (N) and (m). Halpern and Braner use the previous equation for explaining decay of TL as before Adirovitch used for explaining phosphorescence decay, and it says that when heating the sample, the luminescence can be measured, while two states involved one recombination center and one trapping state. Two basic assumptions named quasi-equilibrium assumption for solving the previous set of equations have been made by McKeever and Chen it's the best assumption ever.

$$n_c \ll n \quad , \quad \left|\frac{dn_c}{dt}\right| \ll \left|\frac{dn}{dt}\right| \qquad (3.6)$$

According to assumption of equation 3.6, there is no change in concentration of electron in C.B means $dn_c = 0$, so equation 3.5 becomes

$$n_c = \frac{s\,n\,\exp(-E/KT)}{m\,A_m + A_n(N - n)} \qquad (3.7)$$

$$I(t) = -\frac{dm}{dt} = -\frac{dn}{dt} \qquad (3.8)$$

So we can get the equation of intensity also called general equation for one trapping (GOT), given by

$$I(t) = \frac{n\,s\,\exp[-\frac{E}{KT}]}{m\,A_m + (N-n)A_n} \times m\,A_m \qquad (3.9)$$

From the equation 3.9, we could analytically solve and obtain the equation of first and second order kinetic.

3.1.2 First Order Kinetic

Randall and Wilkins for solving the GOT equation (3.9) analytically assumed that the recombination is dominant means that neglected re-trapping $(mA_m \gg (N-n)A_n)$ so equation (3.9) becomes:

$$I(t) = -\frac{dn}{dt} = sn\,\exp^{\left(-\frac{E}{kT}\right)} \qquad (3.10)$$

The above equation is a differential equation that describes the movement of charge as a process of a first order (b=1) in the lattice, as it's clear the probability $p = \exp(-E/kT)$ is constant when temperature unchanged (constant), so by integration equation (3.10) it can determine intensity:

$$I(t) = I_0 \exp(-p \times t) \qquad (3.11)$$

Where I_0 is called intensity at the prime time. Since if the temperature varies means that also probability and intensity are varied then a solution of equation (3.10) given by:

$$I(t) = -\left(\frac{dn}{dt}\right) = n_0 s\,\exp^{\left\{-\frac{E}{kT(t)}\right\}} \times \exp^{\left\{-s\int_0^t \exp^{\left\{-\frac{E}{kT(t)}\right\}}dt\right\}} \qquad (3.12)$$

Here, n_0 indicating the total number of restricted electrons at $t = 0$, Typically, TL notes as a linear function of time as temperature increased due to

$$T(t) = T_0 + \beta\,t \qquad (3.13)$$

Here β and T_0 heating rate and temperature at $t = 0$ respectively. So as a function of temperature intensity $I(T)$ given by:

$$I(T) = -\frac{1}{\beta}\left(\frac{dn}{dt}\right) = n_0 \frac{s}{\beta} \exp\left\{-\frac{E}{kT}\right\} \times \exp\left\{-\frac{s}{\beta}\int_{T_0}^{T} \exp\left\{-\frac{E}{kT}\right\}dT\right\} \qquad (3.14)$$

In theory for a single glow peak, this is the famous equation of Randall and Wilkins first-order expression. However, the right side of the equation (3.14) in the case of linear heating rate still not integrated easily, but after that Chen presented that by using asymptotic series it can be integrated the right side of this famous equation and evaluated. Kitis et al [28], in actual application, display that equation (3.14) able to approximated pretty accurately, as for describing glow peaks it was appropriate for parameters that are easily experimentally solved it was, given by:

$$I(T) = I_m \exp\left[1 + \frac{E}{kT}\frac{T-T_m}{T_m} - \frac{T^2}{T_m^2}\exp\left\{\frac{E}{kT}\frac{T-T_m}{T_m}\right\}\left(1 - \frac{2kT}{E}\right) - \frac{2kT_m}{E}\right] \qquad (3.15)$$

Randall Wilkins formula (3.14), as in Fig. 3.2, the properties of the graph which the same time explains properties equation 3.14 is given as examples in the article [29]. Firstly, when phenomena of luminescence occur, the intensity increase with rising temperature until reaching the maximum point (increasing intensity due to increasing process of recombination), after that point it will decreases (intensity decreases due to a reduction in the number of carriers at the same time means decrease process of recombination). This is why intensity pattern, it's a peak shape likeness.

From the Figure 3.2a, when some parameter like ($E = 1Ev, s = 1.0 \times 10^{12}s^{-1}$ and $\beta = 1K/s$) are unchangeable then by variation of n_0 from ($n_0 = 0.25m^{-3}$) to ($n_0 = 2m^{-3}$) it can be denoted the difference in intensity. However, at all of the peak, it can be noticed the stability of maximum temperature(T_m), all TL curves of first order have this property. By taking the condition of (dI/dt=0) or ($\frac{d\ln I(T)}{dt} = 0$) can obtain:

$$\left(\frac{\beta E}{kT_m^2}\right) = s \exp\left\{-\frac{E}{kT_m}\right\} \qquad (3.16)$$

T_m is not depend on (n_0) this is why in equation (3.5) (n_0) is not exist. But the proportionality of each point of the curve with (n_0) can be noticed in Figure (3.2a), furthermore in the dosimetry application (n_0) is one of the significant parameters, it can be easily known that (n_0) and area under the curve of glow peak are equal to each other.

$$\int_0^\infty I(t)\,dt = -\int_0^\infty \frac{dn}{dt}\,dt = -\int_{n_0}^{n_\infty} dn = n_0 - n_\infty \qquad (3.17)$$

From the above equation if $(t \to \infty)$ then $(n_\infty = 0)$. For the first order kinetics by [30], the maximum intensity was derived.

$$I_m = n_0 \times \frac{\beta E}{kT_m^2} \times \exp^{(-\frac{E}{kT_m} \exp^{\frac{E}{kT_m}})E_2(x)} \qquad (3.18)$$

Where E_x is the exponential integral of the second order, while from the above equation it could obtain that height of the peak is proportionality depends on n_0 and β respectively.

The changing and increasing of activation energy as shown in Figure (3.2 b) from (0.8 ev) to (1.2ev) make a shifting to a higher temperature in the peak with increase of width and decreasing maximum intensity I_m, but because of (n_0) is unchanged (constant), it could not observe changes in the area. Since if charge carriers are sitting in the dipper level of energy it must gain more energy to be free in the trap and this is the reason for occurring this shifting in the peak. The similar variation could be observed in Figure (3.2c) but at lower temperatures charge, carriers can be free if the center of trapping takes higher values due to changing frequency coefficient in the opposite way, in the first peak this is manifest.

Also, the glow curve shapes are influenced shown in Figure (3.2d) due to the effecting of heating rate on it, it notice the shifting of peak toward higher temperature as β from $\left(0.5\frac{K}{s}\right)$ to $(2\frac{K}{s})$ changed and the height of peak decreases but width increase.

3.1.3 Second Order Kinetics

The assumption which the possibility of re-trapping $(m\,A_m \ll (N - n)A_m)$ is dominant was demonstrated by Garlik and Gibson [31], also they assumed the away of the trap from the saturation $((N \ll n)$ and $(n = m))$. According to this assumption, the solution of GOT equation (3.9) becomes:

$$I(t) = -\frac{dn}{dt} = s\,\frac{A_m}{NA_n}n^2\,\exp^{\{-\frac{E}{kT}\}} \qquad (3.19)$$
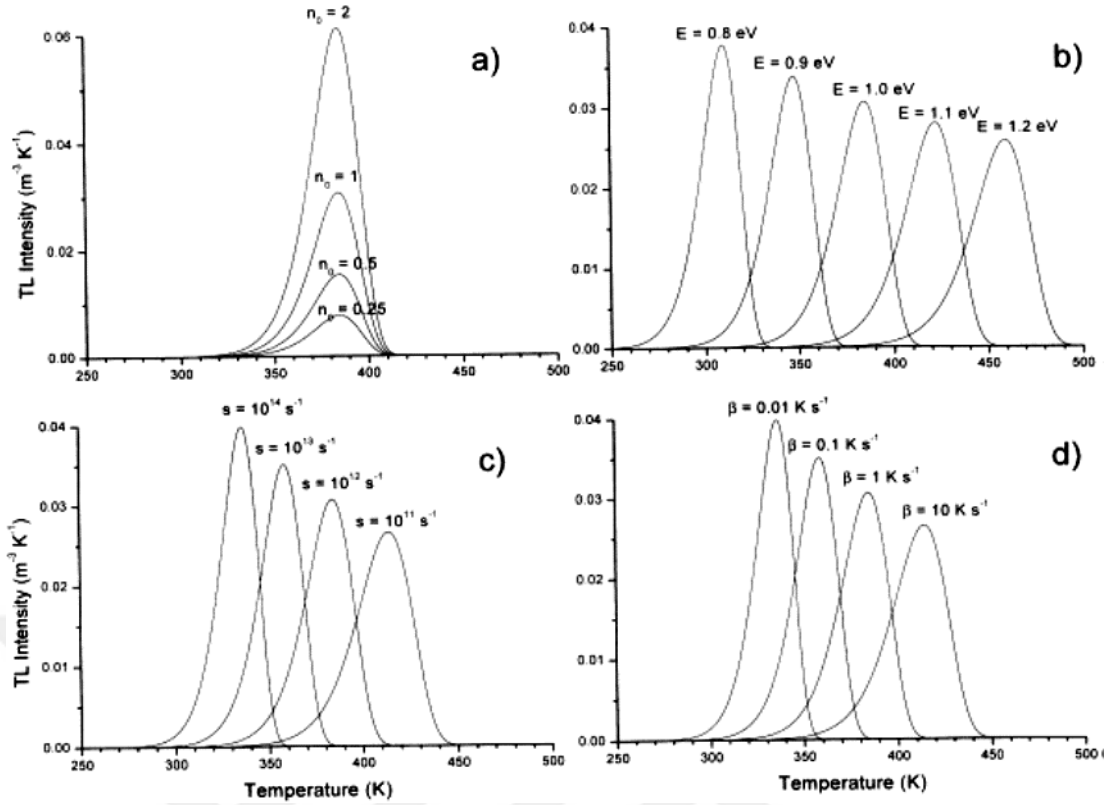
Figure 3.2 Properties of the Randall and Wilkins first-order thermoluminescence (TL) equation, showing variation with; (a) the trapped charge carriers concentration after irradiation (no), (b) activation energy (E), (c) the escape frequency (s), and (d) the heating rate (β). Parameter values: (n_0 = 1m^{-3}) (E=1eV) (s=1×10^{12}s^{-1}), of which one parameter is varied while the others are kept constant, and (β =1 K/s) for (a, b, and c) [29].

The proportionality between dn/dt with n^2 can be observed from the equation (3.19) which refer to a second order reaction, and by assuming the assumption equality of probability of recombination and re-trapping ($A_m = A_n$), of course by unchanging temperature, the previous equation by some mathematical solution becomes [29]:

$$I(T) = \frac{n_0^2}{N}\frac{s}{\beta}\ exp^{\{-\frac{E}{kT}\}}\ \left[1 + \frac{n_0 s}{N\beta}\int_{T_0}^{T} exp^{\{-\frac{E}{kT}\}}d\acute{T}\right]^{-2} \qquad (3.20)$$

This is an equation for a second-order kinetic that was titled by the Garlick-Gibson TL equation.

The shape of the glow curve in Figure (3.3a) can be seen is almost symmetric, but can notice a difference in the part end of the curve, it's clear at high temperature broader than the initial of the curve in lower temperature.

The reason of wider curve due to the consideration of the second order reaction suggested that before recombination process occurs concentration of released electron are re-tapped and emission of a photon (luminescence) delayed and at a wider temperature this emission spread.

In the case of first-order kinetics n_o is not affected by the shape of the curve because it's constant but in this case and in various dose level n_o is influenced by the form of the curve, and in Figure (3.3a) can be seen by changing (n_o), T_m also varying, it can be determined that the temperature displacement [32].

$$T_1 - T_2 \approx T_1 T_2 \left(\frac{k}{E}\right) \ln f \tag{3.21}$$

T_1 at a specific dose is the temperature at maximum intensity and for a higher dose T_2 at times (f) is the temperature of the maximum intensity. From this equation by a certain increase of the dose can notice the trap shallower.

The influence of parameters E, s/N, and β respectively on the variation of second order peak in position and size in Figure (3.3 b, c, and d) are explained. Area under the glow curve it is similar to the first order kinetic means proportional to n_0 but with a height of the peak is not proportional anymore.

To find the depth of the trap, even if the similarity of the first and second use is "initial rise method" since the term dominance is temperature dependency in the initial rise is $(\exp^{-E/kT})$. The first order kinetic can be approximately written Garlics-Gibson thermoluminescence (TL) equation as a function of maximum intensity (I_m) and temperature (T_m) for a first-order kinetics [28].

$$I(T) = 4I_m \exp\left(\frac{E}{kT}\frac{T-T_m}{T_m}\right) \times \left[\frac{T^2}{T_m^2}(1-\Delta)\exp\left\{\frac{E}{kT}\frac{T-T_m}{T_m}\right\} + 1 + \Delta_m\right]^{-2} \qquad 3.22$$
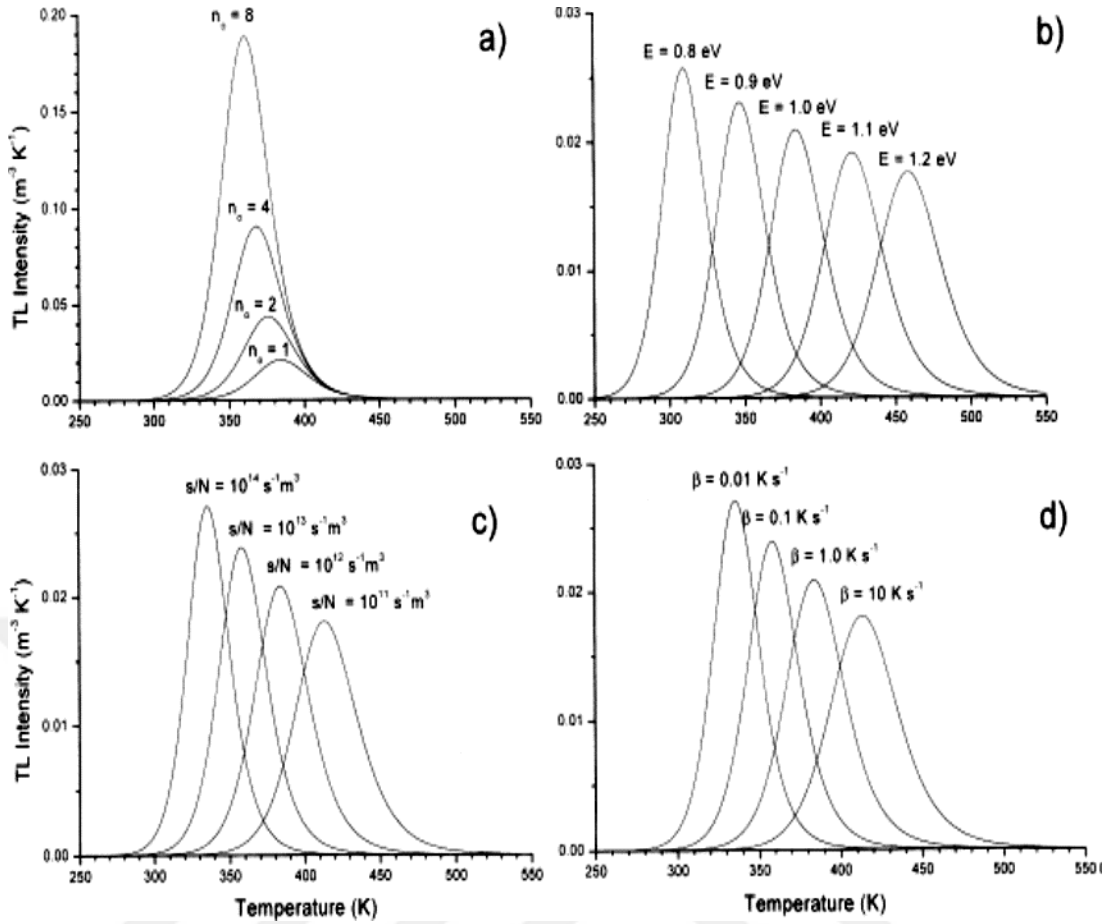
Figure 3.3 Properties of Garlick–Gibson second-order TL equation, showing variation with: (a) the trapped charge carrier concentration (no) after irradiation; (b) activation energy (E), (c) (s/N), and (d), the heating rate (β). Parameter values: $(n_0=1m^{-3})(E=1eV)$ $(s/N=1\times10^{12}s^{-1}m^3)$, of which one parameter is varied while the others are kept constant, and (β =1 K/s) for (a, b, and c) [29].

3.1.4 General Order Kinetics

First and the second-order reaction of TL equation in a previous section by utilizing several simplifying assumptions have been concluded. However, in fact, thermolumin-escence peak neither the first nor the second-order will not fit because these simplifying assumptions don't hold experimentally. May and Partridge [33] in the case of general order kinetics utilized an experiential expression is:

$$I(t) = -\frac{dn}{dt} = n^b \, \acute{s} \, \exp^{-\frac{E}{kT}} \tag{3.23}$$

Where the dimension of (s') is ($m^{3 \,(b-1)} s^{-1}$) and parameter (b) is defined as general order parameter and this parameter if it is equal to (1) or (2) or not equal it's not necessary for here. For above equation, when (b≠1) by integrating it becomes:

$$I(T) = \frac{s''}{\beta} \, n_0 \, \exp^{\{-\frac{E}{kT}\}} \left[1 + (b-1)\frac{s''}{\beta} \times \int_{T_0}^{T} \exp^{\{-\frac{E}{kT}\}} d\hat{T}\right]^{\frac{-b}{b-1}} \tag{3.24}$$

Where $s'' = s' \, n_0^{(b-1)}$ in the unit (s^{-1}), equation (3.24) is a general equation and can be changed to first and second-order when (b=1) and (b=2) respectively, s' has a dimension due to equation (3.23) and with respect to the order (b) is changed. So in this case as its clear in Figure (3.4) can be dealt as the first order when $b \to 1$ and when $b \to 2$ go to the second order:
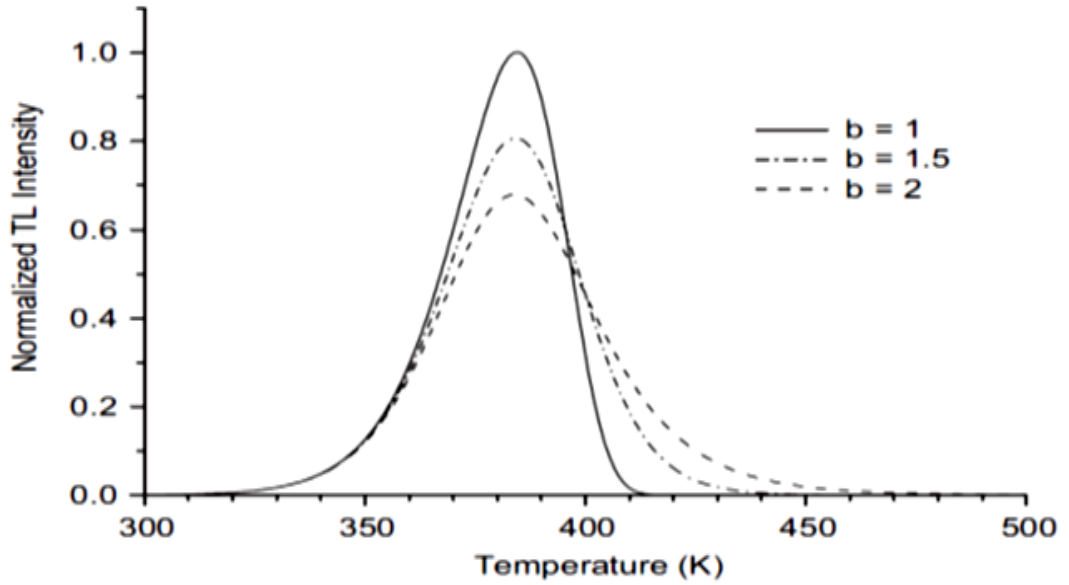
Figure 3.4 Comparison of first (b=1), second (b=2), and intermediate-order (b=1.5) [43].

The variation temperature represents as:

$$T_1 - T_2 \approx T_1 T_2 \left(\frac{k(b-1)}{E}\right) \ln f \tag{3.25}$$

At a certain dose expression T_1 is temperature for maximum intensity and at (f) times higher dose T_2 is the temperature of extreme intensity. And the equation of general-order in term of I_m and T_m can be written, that derived [34].

26

3.2 Methods and Analysis of the Trapping Parameters

As its clear finding the thermoluminescence parameter it's so important, and generally, it has four thermoluminescence parameters. After the successful working of Randall & Wilkins with Garlic & Gibson, many researchers improved and worked on their studies with the method of analysis. In this chapter for finding parameters briefly will be discussed some methods. However, the first 2 parameters that also called trapping parameter (activation energy E_a and frequency factor S) can be evaluated from the glow curve this way it was obtained in the last mid-century, now for determining trapping parameter; there are numerous methods for evaluating parameter from the glow curve [5,35,36]. The other two parameters can experimentally determine by choosing certain dose (n_0) as well as through the reading of the signal at a certain heating rate (β). Due to the situation of the peaks, the method that used for determining is different if single glow peak separated from the other usually the experimental method example initial rise, three-point, peak shape, heating rate, and isothermal decay are applied. And if the peaks are overlapping each other in this case the method of partial thermal cleaning and computer glow curve deconvolution method are used but because of in most case thermal cleaning method without any perturbation can't be used for isolation peaks so in recent year CGCD method it was so popular way for determining trapping parameter from the glow curve.

3.2.1 Heating Rate Method

The various heating rate methods are important techniques for determining the activation energy, and it goes without saying that the differences in the heating rate (β_1) and (β_2), when heating the sample have peak shapes or (I_m maximum Temperature) are different. By using equation 3.26 and can be written for each heating rate, then by dividing equation (β_1 and T_{m1}) of the formula (β_2 and T_{m2}) and arrange it, is an obvious equation (3.26) for the calculation of activation energy (E) obtained shown in equation 3.27.

$$\frac{\beta E}{kT_m} = s \exp^{(-\frac{E}{kT})} \tag{3.26}$$

$$E = k \frac{T_{m1} T_{m2}}{T_{m1} - T_{m2}} \ln\left[\left(\frac{\beta_1}{\beta_2}\right)\left(\frac{T_{m2}}{T_{m1}}\right)^2\right] \tag{3.27}$$

The basic feature of this method is that it is necessary to take data with the peak maximum value (T_m, I_m), and in the case of a large peak surrounded by a small satellite, accurately and precisely determined from the glow curve can do. Furthermore, the problem due to thermal quenching does not affect the calculation of (E) as in the Initial Rise Method (IRM). However, there are some difficult approaches to determining (E) of smaller peaks. There are also other processes for finding (I_m, T_m).

When using various heating rates for first-order kinetic, yields the following equation:

$$\ln\left(\frac{T_m^2}{\beta}\right) = \left(\frac{E}{k}\right)\left(\frac{1}{T_m}\right) + \text{canstant} \qquad (3.28)$$

The straight line with slope equal to (E / K) obtain by plotting $\ln(T_m{}^2/\beta)$ versus (1 / T). Therefore, evaluate of (E) it is possible to do. Furthermore, extrapolation to $(1/T_m = 0)$ gives the value of (ln(s K/E), by inputting the value of (E / k) obtained from the slope can calculate the frequency coefficient (s). Different heating rate methods it's also applicable methods to general kinetics including second-orders. $((\ln[I_m^{b-1}(T_m^2/\beta)^b]))$ can be plotted against $(1/T_m)$, its slope is equal to (E / k).

3.2.2 Peak Shape Method

In peak shape method for determining the kinetic parameter (b, E_a, s) is dependent on the shape of the glow peak which is selecting three points on the glow peak $(T_m, T_1, \text{and } T_2)$, T_m is the maximum temperature at the maximum point of intensity (I_m). T_1 and T_2, are the half height of low temperature and half height of high temperature respectively shown in Figure (3.5). After selecting these three points it can be used for finding another parameter like $\omega = T_2 - T_1$, $\delta = T_2 - T_m$, $\tau = T_m - T_1$, and $\mu_g = \frac{\delta}{\omega}$ which is called shape or geometry parameter. These parameters help to find the trap parameters example due to parameter μ_g it can be found the kinetic order (b) but Chen [38] found that μ_g is not sensitive to (E_a) and (s), in a case of the linear heating rate it's shown that the variation of range μ_g from (0.42) which (b=1) to (0.52) which (b=2) as shown in Figure (3.6).
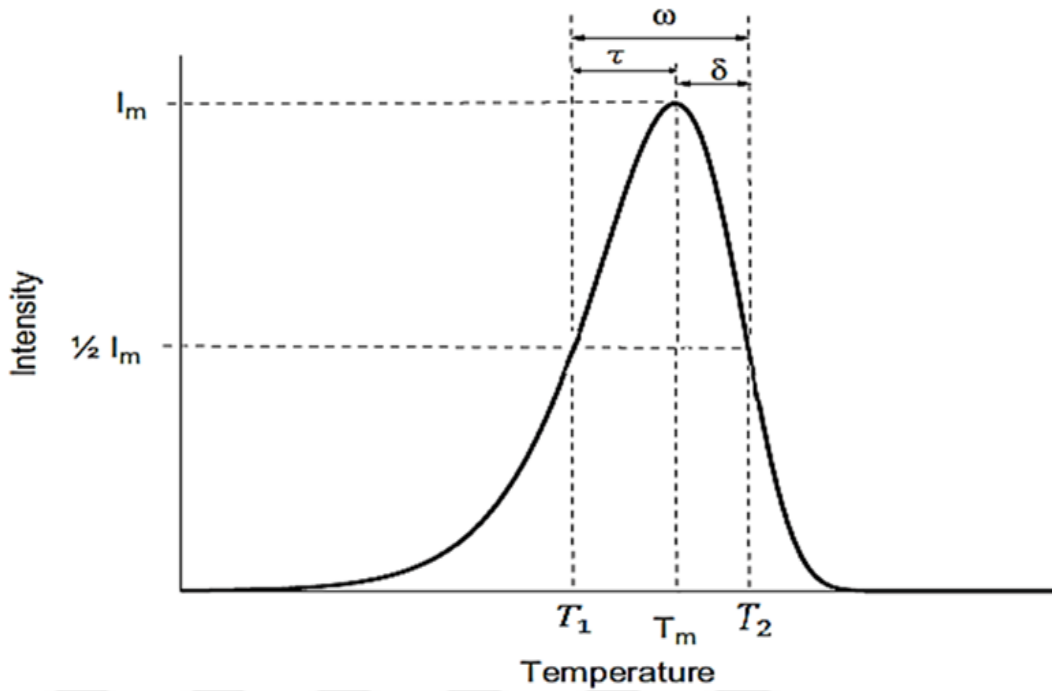
Figure 3.5 Normalized glow peak and shows characteristics of a single glow peak with defining the peak shape parameters [49].
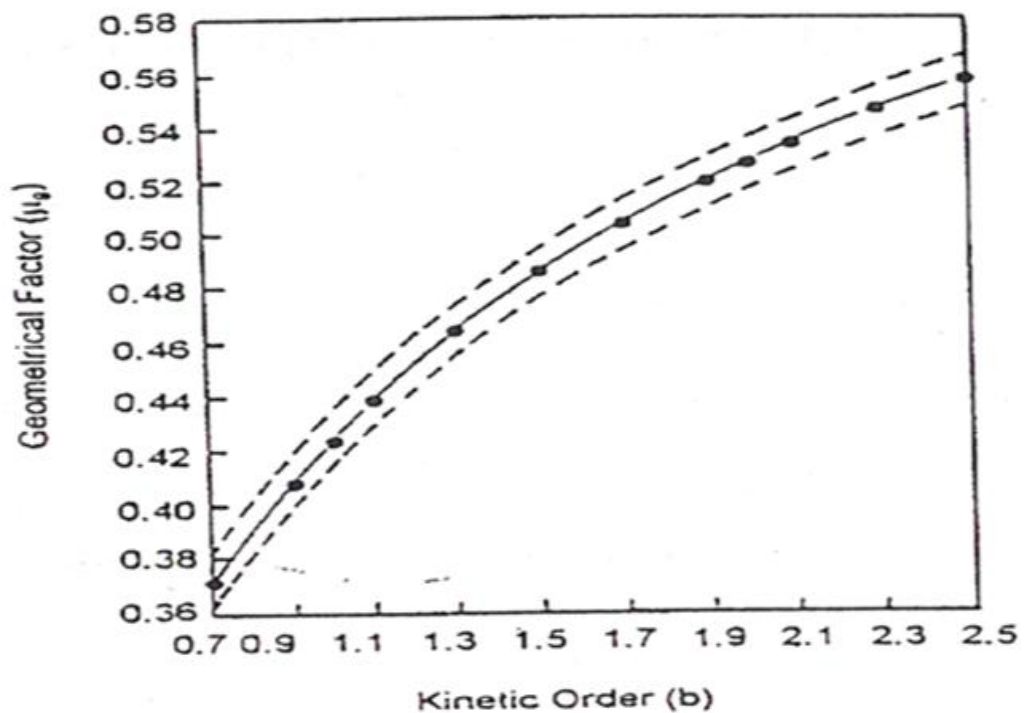

Figure 3.6 Geometrical factors (μ_g), as a function of the given order [37].

The first (PS) method was improved by the Gross Weiner [38], later the equation of Halpern and Burner's equations was reformulated [39] to evaluating activation energy (E_a),

$$E_\tau = \left[1.51 + 3(\mu_g - 0.42)\right]\frac{kT_m^2}{\tau} - \left[1.58 + 4.2(\mu_g - 0.42)\right]2kT_m$$

$$E_\delta = \left[0.976 + 7.3(\mu_g - 0.42)\right]\frac{kT_m^2}{\delta} \tag{3.29}$$

$$E_\omega = \left[2.52 + 10.2(\mu_g - 0.42)\right]\frac{kT_m^2}{\omega} - 2kT_m$$

After evaluating the kinetic order and due to the previous equations calculate activation energy, then by using the following expressions frequency factor can be evaluated, this parameter in the general order kinetic named as a pre-exponential factor.

$$s = \frac{\beta E}{kT_m^2}\exp\left[\frac{E}{kT_m}\right]$$

$$s = \frac{\beta E}{kT_m^2}\left[\exp^{(-\frac{E}{kT_m})(1+\frac{(b-1)\,2kT_m}{E})}\right]^{\frac{b}{b-1}} \tag{3.30}$$

In addition, Chen's equations also modify by Garcia, Singh & Mazumdar [40], which is more accurate can determine activation energy and also on a peak can choose three points, the form of this equation as follows

$$E_a = \frac{(C_0 + C_1 + C_2 b^2)kT_m^2}{|T_x - T_y|} + (D_0 + D_1 b + D_2 b^2)kT_m \tag{3.31}$$

Where $|T_x - T_y| = \tau, \delta, \omega$, and the coefficients ($C_0, C_1, C_2, D_0, D_1,$ and D_2) are shown in Table 3.1 which from the least squares method for kinetic order range (b=0.7 to 2.5) and x=1/2, 2/3, and 4/3 are obtained.

Table 3.1 Numerical values of the coefficients comparing in equation (3.31) [40].

Ratio	Parameter	C_0	C_1	C_2	D_0	D_1	D_2
1/2	τ	1.019	0.504	-0.066	-1.059	-1.217	0.109
	δ	0.105	0.926	-0.048	0.154	-0.205	-0.128
	ω	1.124	1.427	-0.113	-0.902	-0.346	-0.061
2/3	τ	0.684	0.426	-0.055	-0.720	-1.21	0.098
	δ	0.146	0.683	-0.048	0.184	-0.432	-0.094
	ω	0.830	1.108	-0.103	-0.529	-0.607	-0.029
4/5	τ	0.449	0.342	-0.043	-0.0480	-1.184	0.085
	δ	0.153	0.487	-0.041	0.180	-0.606	-0.062
	ω	0.602	0.829	-0.084	-0.293	-0.777	-0.006

3.2.3 Computer Glow Curve Deconvolution (CGCD) Method

One of the most important way that use for obtaining the value of the parameter E_a, s, and b is the Computer Glow Curve Deconvolution (CGCD) method, and instead of heating and adding addition doses by CGCD method can separate many overlapping glow peaks, these computerized curve fitting methods are more accurate with clearly successful value in use.

The procedure of this method is firstly from the glow curve the approximation locations of the most evident peak is finding and by using one of the analytical methods is estimated each value of Ea, s, and b. Also the theoretical curve by using one of the equations of (general-order ($b \neq 1$)) or (first-order ($b = 1$)) equations calculated. The computed curve with the exact result of the experimental curve is compared. Between the two results, the method of root means square is applied.

This method is useful and better than experimental method because without acting to heat treatment can be used in the largely overlapping peak of glow curve [44].

Two different patterns it utilized in this computer program in the first pattern is approaching of glow curve to the first order thermoluminescence kinetics is following:

$$I(T) = n_0 s \, \exp\left(-\frac{E}{kT}\right) \exp\left[\left(-\frac{s \, kT^2}{\beta \, E} \exp\left(-\frac{E}{kT}\right)\right) * (0.9920 - 1.620 \frac{kT}{E_a})\right] \tag{3.32}$$

In the second pattern is approaching of glow curve to the general order thermoluminescence kinetics is following:

$$I(T) = n_0 s \, \exp\left(-\frac{E}{kT}\right) \left[1 + \left(-\frac{(b-1)s}{\beta} \frac{kT^2}{E} \exp\left(-\frac{E}{kT}\right)\right) * (0.9920 \right.$$

$$\left. - 1.620 \frac{kT}{E_a})\right]^{\frac{b}{b-1}} \tag{3.33}$$

The summary of the total peak and the background can lead to the formula of the composite glow curve as follows:

$$I(T) = \sum_{i=1}^{n} I_i(T) + a + b \, \exp^{(T)} \tag{3.34}$$

If $I(T)$ is the adjusted total glow curve, (a) it enables the electronic noise contribution plant and the infrared background of the dosimeter.

In equation 3.31 by use the least-squares minimization procedure and the Merit (FOM) figure to determine the appropriate result depending on either they are good or not, like:

$$FOM = \sum_{i=1}^{n} \frac{|N_i(T) - I(T)|}{A} = \sum_{i=1}^{n} \frac{|\Delta N_i|}{A} \tag{3.35}$$

I (T) is the (i-th) fitting point, (A) is the integral region of the settled glow curve, where $N_i(T)$ is the (i-th) experimental point (total number $n = 200$ data points). In the study of the FOM value, the three states were obtained [41, 42]. These are 0.0% to 2.5%, the adjustment is good, 2.5% and 3.5%, the adjustment is fair and the corresponding values of $> 3.5\%$ are poor.

To obtain a match between the adjusted glow curve and the experimental results, the graphical representation is plotted by a computer program that has the following equation:

$$X(T) = \frac{N_i(T) - I_i(T)}{\sqrt{I_i(T)}}$$
(3.36)

In the above equation it is a natural variable value (0) and ($\sigma = 1$) where ($\sigma^2(T) = I_i(T)$) was expected.

The computerized glow curve deconvolution (CGCD) method has become very popular way to obtain the kinetic parameters from the glow curves of TL materials [61,62]. Therefore, the kinetic parameters such as number of glow peaks, activation energies (E_a), frequency factor (s) and kinetic order (b) for the dosimetric peaks of $Ba_2SiO_4:Dy^{3+}$ were obtained by CGCD method. In this study, the following general order kinetic analytical equation was used by the approximation for b≈1.1 [63].

$$I(T) = I_m \cdot b^{b/b-1} \cdot \exp\left(\frac{E}{kT} \cdot \frac{T - T_m}{T_m}\right)$$
$$\cdot \left[(b-1) \cdot (1-\Delta) \cdot \frac{T^2}{T_m^2} \cdot \exp\left(\frac{E}{kT} \cdot \frac{T - T_m}{T_m}\right) + Z_m\right]^{-b/b-1}$$

where;

$$\Delta = \frac{2kT}{E} \quad , \qquad \Delta_m = \frac{2kT_m}{E} \quad , \quad Z_m = 1 + (b-1) \cdot \Delta_m$$

The number of glow peaks is not a free fitting parameter during the deconvolution of the measured glow curve into individual components in the CGCD programs. If the number of peaks is not known, it can be found by fitting the glow curve several times with a different number of components up to obtaining best-fit result. In this study, after many tries with different number of glow peaks, it was observed that the glow curve structures of $Ba_2SiO_4:Dy^{3+}$ are well described by a linear combination of at least five glow peaks. In this case, a reasonably good fit was always obtained.

CHAPTER 4

EXPERIMENTAL PROCEDURE

In this chapter, it's described the experimental procedure, equipment, and the way that material achieved and produced.

4.1 Experimental Procedure and Equipment

4.1.1 Irradiation Process and Radiation Source

In this action, during the experiment, beta rays ^{90}Sr - ^{90}Y was used as a radiation source Figure 4.1. Beta radiation source ^{90}Sr - ^{90}Y together with opened cover has been placed on a special lead block. In this system the sample was irradiated for 1 sec. Any material can be irradiated in any interval time by using the computer controlled system.

Figure 4.1 Radiation sources of beta ray ^{90}Sr - ^{90}Y source (≈ 0.04 Gy/s).

In the experiment, the specimen was irradiated at a temperature 27 °C (room temperature) by a beta ray from a calibrated emitter ^{90}Sr - ^{90}Y Fig 4.1. Strontium -90 from their daughter products (^{90}Sr β -0.546 MeV together with ^{90}Y β -2.27 MeV) emits high energy beta particles. Beta radiation is ionized by air caused an absorbed by air, means with distance reduction in intensity could notice much more rapidly than inverse square law calculation indicates. Beta particle Y-90 in the air has a maximum influence area 9 meter approximately. The typical strength of a 100 mCi Sr-90 beta source installed in a 9010 optical dating system is 3.3 Gy/min = 0.055 Gy/sec for 100 m quartz on stainless steel, or 2.64 Gy/minute = 0.0438 Gy/sec for fine grain on aluminum. The irradiation equipment which is purchased from little more scientific engineering UK [45] is a computer part of the 9010 optical dating system. All experimental process in dark room was executed to avoid the effect of the external light on the glow curve.

4.1.2 System TLD Reader and Process of Emission

In this experiment, Harshaw QS 3500 TLD reader system was used to read out the irradiated sample. This system is a manual type reader which is computer interfaced to hand operator in Figure 4.2, TLD reader system and program that run on WinREMS (Windows Radiation Evaluation and Management System).

Figure 4.2 QS 3500 Harshaw TLD reader.

In this system, the test site is designed for one sample. There is a typical transparent glass filter between the conductor plant and the photomultiplier tube to avoid the affecting infrared radiation on the reader. During heating, PMT (Photo Multiplier Tube) is used to detect luminescence of the sample. By increasing the emissions and using the computer program with WinREMS, signals from the PMT are displayed and recorded.

During operation, after the irradiation process, the irradiated sample was placed in the tray and heated. The irradiated samples were then read with a reader, and the TL signal was obtained on a WinREMS computer. The program to solve a separate peak of the glow curve, get the best value. The luminescence curve was measured from room temperature to 400 ° C with a linear heating rate of 1 ° C / s. Schematic diagram of the TL reader is shown in Figure 4.3.
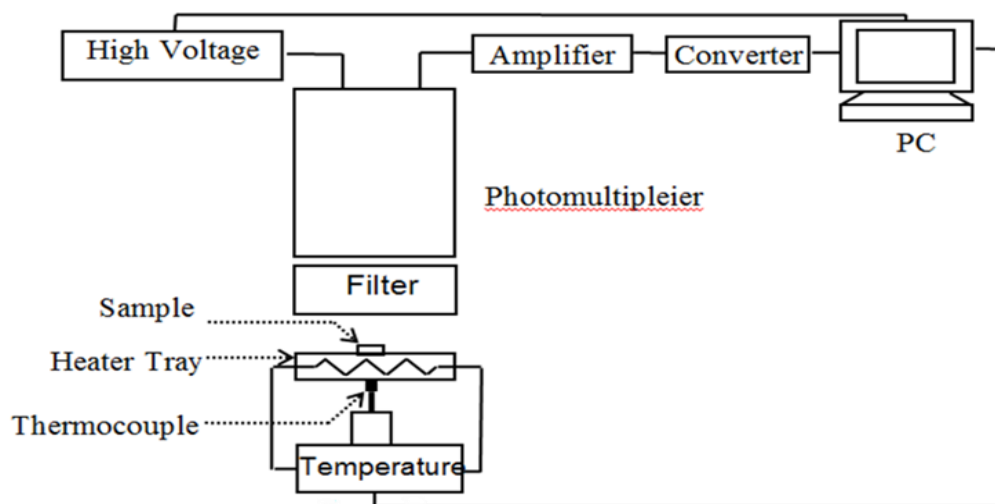

Figure 4.3 Essential scheme diagram of TL reader [43].

The WinREMS program has a Time-Temperature Profile (TTP). It consists of three pieces each with independent times: preheating, acquisition and annealing, (pre-read annealing: adjustable from 0 to 1000 sec, linear ramp: adjustable from 1 ℃ to 50 ℃ per second, annealing after recording: 0 to 1000 Sec) and temperature (pre-read annealing temperature up to 200 ℃, consequent annealing: up to 400 ℃). Figure 4.4 shows a typical Time-Temperature Profile (TTP). Nitrogen is assigned to the area of the planchet in order to extend the lifetime of the plant and increase the accuracy of

signs of low exposure. Also to remove moisture formed during condensation through the Photo Multiplier Chamber (PMT), for this purpose the nitrogen is used.
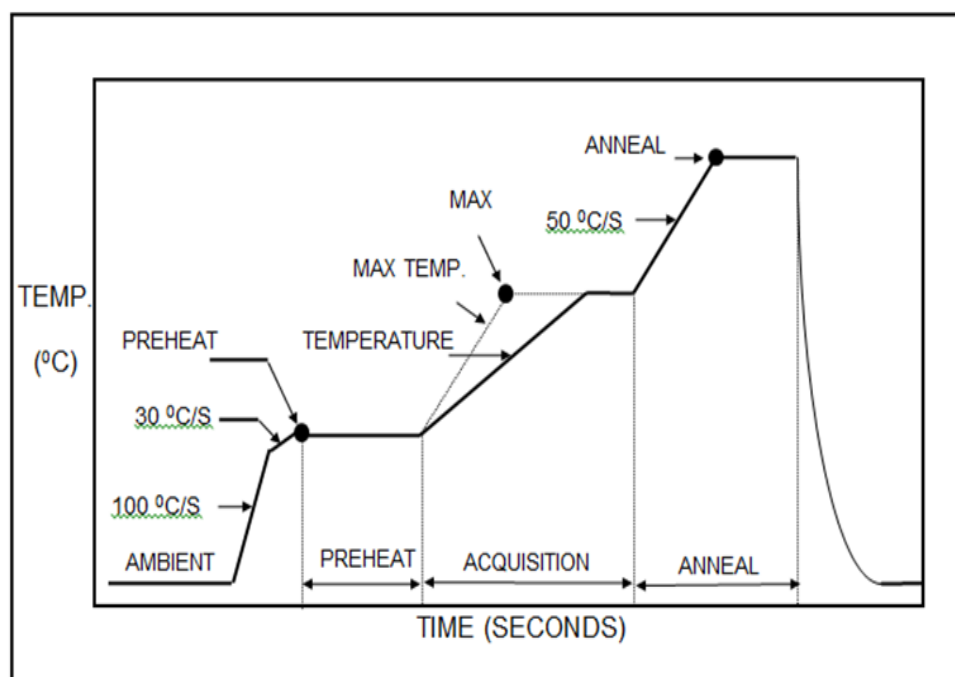

Figure 4.4 Typical time-temperature profile (TTP) [45].

4.2 Synthesis of Dysprosium doped Barium Silicate (Ba$_2$SiO$_4$: Dy^{3+}).

$2,6\times10^{-3}$ mol Ba(NO$_3$)$_2$ in 15 ml of purified water, 2×10^{-3} mol SiO$_2$.xH$_2$O in pure water or TEOS (twice the molar ratio of polyethylene glycol with TEOS will be used) in 15 mL ethanol and 0.2 g citric acid in 10 mL pure water were dissolved separately. Dy^{3+} nitrate salts were dissolved in 5 mL of purified water. The solutions of the metal salts mixed with the citric acid solution. Then Ba (NO$_3$)$_2$ solution was added and the mixture was stirred with a magnetic stirrer at room temperature for 10 min. The pH of the homogeneous solution adjusted to 12 with 5 M NaOH and mixed before taking up the hydrothermal reactor. PH adjustment done used PH meter. After the mixture been put into the Teflon reactor left for 1 hour and taken to the hydrothermal unit. The temperature is set at 120-180 °C and held at high pressure for 12-18 hours. After cooling the hydrothermal reactor to room temperature, the precipitate is separated by centrifugation and dried at 60 °C for 12 hours. Ba$_2$SiO$_4$: Dy^{3+} is baked for 3 hours at the required temperature (1250-1350 °C).

CHAPTER 5

EXPERIMENTAL RESULTS

Alkaline earth silicates have been studied by several researchers as useful luminescent hosts with a stable crystal structure and high physical and chemical stability [55, 56]. Different silicate hosts have various effects around activator ions [55]. Alkaline earth metal (Ca, Sr, Ba) silicate attracts a great deal of attention as there is a relatively wide band gap suitable for the sustained luminescent center of Eu^{2+} and Ce^{3+} [53,54], and it has several reports which dealing with the luminescent studied about Sr_2SiO_4, $Ca_2MgSi_2O_7$, $Sr_2MgSi_2O_7$, $Sr_3MgSi_2O_8$ and $Ca_3MgSi_2O_8$ in literature [57,58,59]. However, few journalists treat Ba_2SiO_4 as TL material. In this study we have investigated, it deals with the thermoluminescence properties of dysprosium doped barium silicate (Ba_2SiO_4), and trap parameters were determined using different methods.

In this study, first of all, the structure of Ba_2SiO_4: Dy^{3+} was characterized by X-ray powder diffraction (XRD), in the range of diffraction angle $20° \leq 2\Theta \leq 70°$ using a $0.021°$ with 20 kV at 40 mA, $CuK\alpha$ (1.54A°) radiation using a Rigaku RadB diffractometer. The x-ray diffraction patterns (XRD) of the Ba_2SiO_4:Dy^{3+} (synthesized at 1100 °C) are shown in Figure 5.1 the pattern indexed as a major phase Ba_2SiO_4 (PDF: 01-077-0150) has orthorhombic crystal system with Pmmm space group and unit cell parameters of (a=5.772, b=10.225, c=7.513) A°; $\alpha= \beta =\gamma=90°$.

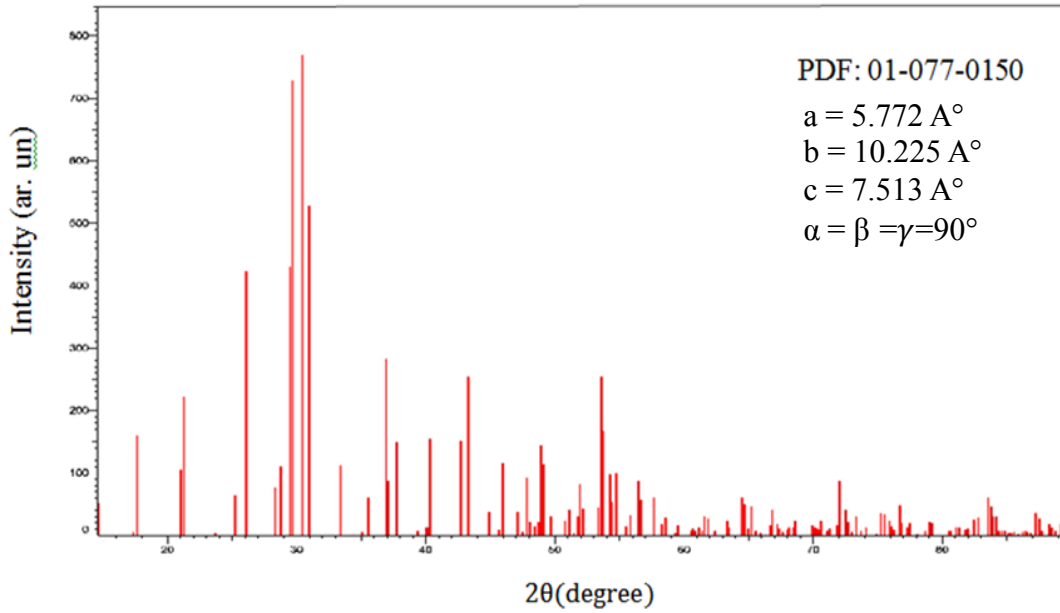**Figure 5.1** XRD patterns of the Ba_2SiO_4:Dy^{3+} phosphor.

The surface morphology of Ba_2SiO_4: Dy^{3+} phosphor synthesized using hydrothermal technique was observed through SEM image analysis and these micrographs are given in Figure 5.2. SEM micrographs with 10000X magnification indicate that average grain size in the obtained (Ba_2SiO_4:Dy^{3+}) phosphor are in the range of 230-650 nm and micro-structures of the phosphors consisted of regular fine grains.

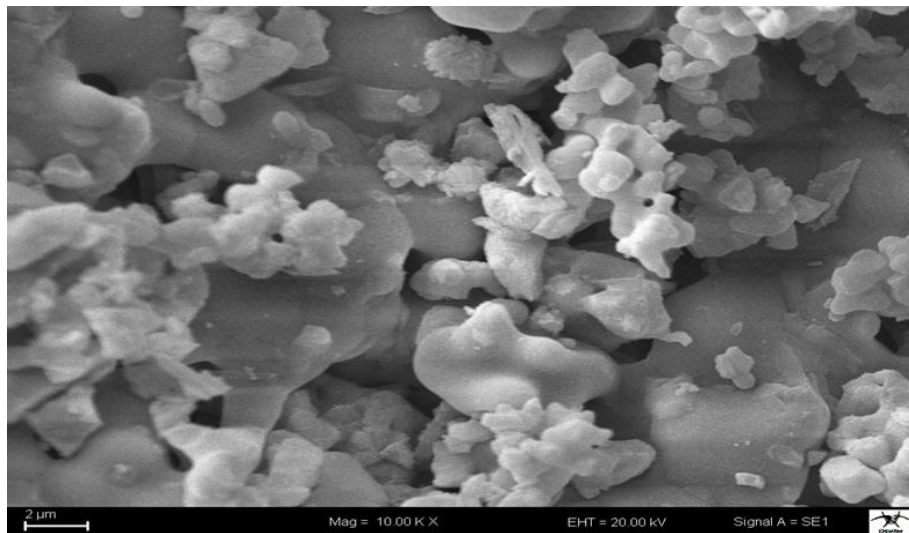**Figure 5.2** SEM micrographs of the Ba_2SiO_4:Dy^{3+} phosphor.

The Dy^{3+} ions belong to the charge transfer transitions between the intense and broadband 0^{2-}—Si^{4+} in the excitation spectrum of the doped Ba_2SiO_4:Dy^{3+} compound in the range of 220-325 nm.

39

The weak excitation bands in the range of 325-400 nm correspond to electron transitions of Dy^{3+} ions from $^6H_{15/2} \rightarrow ^4M_{17/2}$, $^6H_{15/2} \rightarrow ^4M_{15/2}$, $^6H_{15/2} \rightarrow ^6P_{7/2}$, and $^6H_{15/2} \rightarrow ^4I_{11/2}$. The intense emission bands observed at 490 and 590 nm in the radiation spectrum belong to the $^4F_{9/2} \rightarrow ^6H_{15/2}$ and $^4F_{9/2} \rightarrow ^6H_{13/2}$ transitions of Dy^{3+} ions. Furthermore, low-intensity emission bands observed between 650-800 nm belong to the transition of $^4F_{9/2} \rightarrow ^6H_j$ (j=11/2, 9/2) of Dy^{3+} ions shown in Figure 5.3.
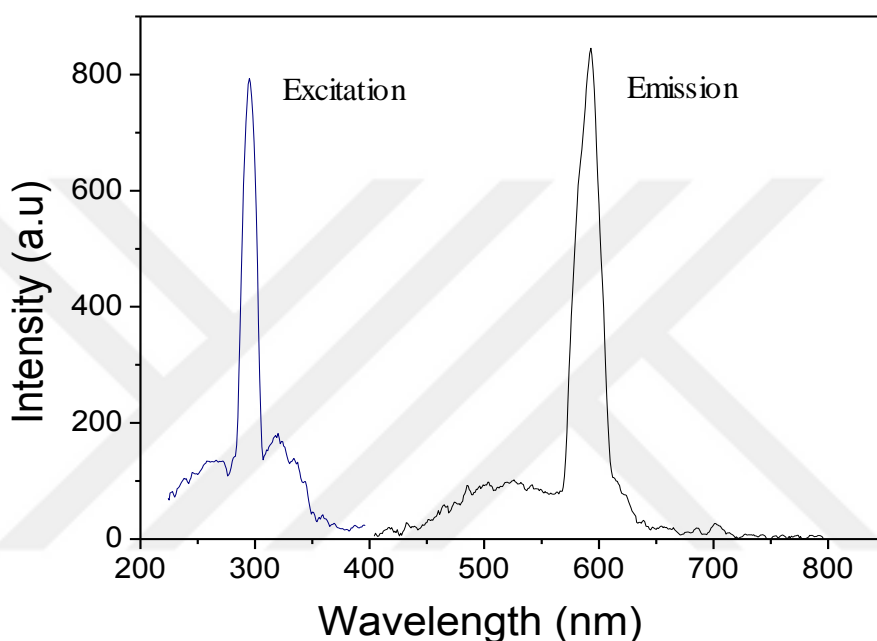

Figure 5.3 Emission spectrum of barium silicate (Ba_2SiO_4:Dy^{3+}).

Also in this study, one of the important ways that were used to find out the dose-response behavior of the (Ba_2SiO_4: Dy) is the different dose levels. The experiment conducted to investigate the effect of dose dependence at a peak position, and for this aim between (2 sec $\approx$ 0.08 Gy to 8-hour $\approx$ 1152 Gy) by β-ray source invariably 15 mg of the sample (that was in powder form) irradiated at room temperature and immediately readout. Figure 5.4 to 5.8 show the glow curve structures of (Ba_2SiO_4: Dy) after different dose levels. In general, experimental tests showed that there was no major shift in the site of peak temperature and there is a slight change in temperature with increasing dose level. That is, the glow peak temperature gradually shifted to the higher temperature side as the dose level increased. Every peak reaches a maximum intensity at around (100 ° C to 150 ° C) at different dose levels and in these figures, the increase or decrease of the height peak relative to the shift dose is also shown.

There are several experimental techniques such as (Initial Rise (IR), Variable Heating Rate (VHR) and Peak Shape (PS)) method as interpreted in section (3.2) for single glow curve to evaluating trapping parameter.

In this study, the method of (peak shape, heating rate, and CGCD) method has been applied for evaluating trapping parameter of the main dosimeter peak of (Dy) doped Ba_2SiO_4. In this part for estimating the value of trapping parameter, the peak shape method was utilized. Previous studies have shown that the evaluation of the activation energy and the frequency coefficient depends mainly on knowledge of the kinetic order (b) and that the glow peak depends on the correct number of glow curves [46]. Therefore, first to find geometry factor used (maximum temperature, T_1, T_2), as explained in section (3.2.2), to find the kinetic order to (72 Gy), and was found that nearly equal to (2) that means in the range of second order kinetics. Activation energy and frequency factor(S) were then determined using Chen peak shape equation (3.29), Mazumdar peak shape formula (3.31), and all values are shown in Table 5.1.

Figure 5.4 Glow curve of Ba_2SiO_4:Dy^{3+} measured after different exposure dose levels (0.08 and 0.2) Gy with ($\beta = 1°C/s$).
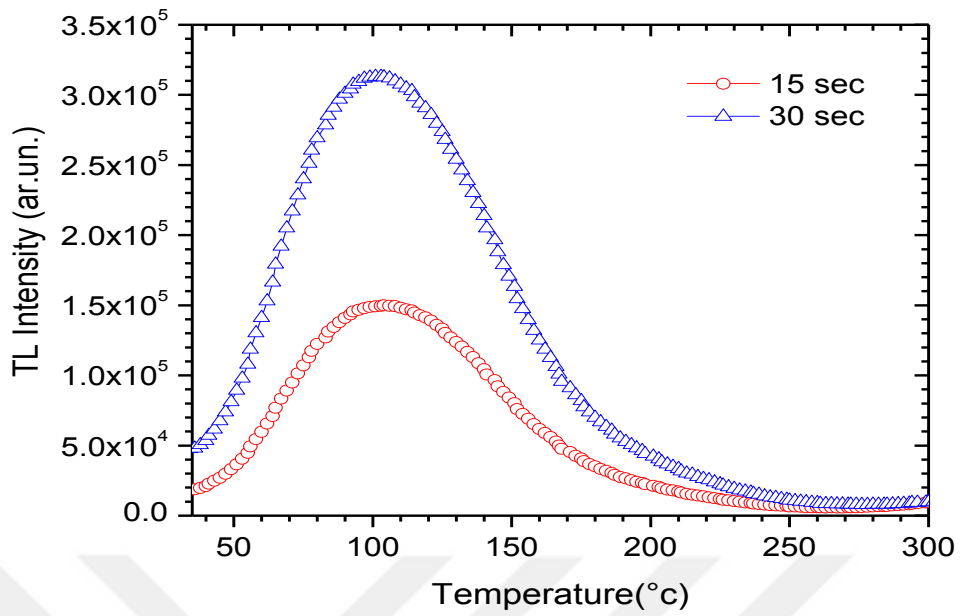
Figure 5.5 Glow curve of $Ba_2SiO_4:Dy^{3+}$ measured after different exposure dose levels (0.6 and 1.2) Gy with $(\beta = 1℃/s)$.
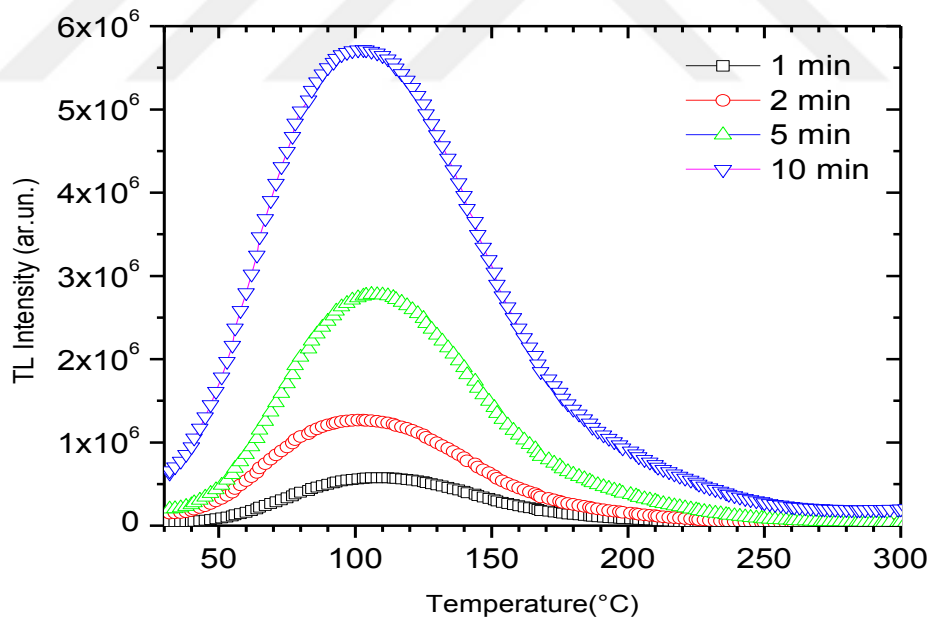
Figure 5.6 Glow curve of $Ba_2SiO_4:Dy^{3+}$ measured after different exposure dose levels (2.4, 4.8, 12, and 24) Gy with $(\beta = 1℃/s)$.
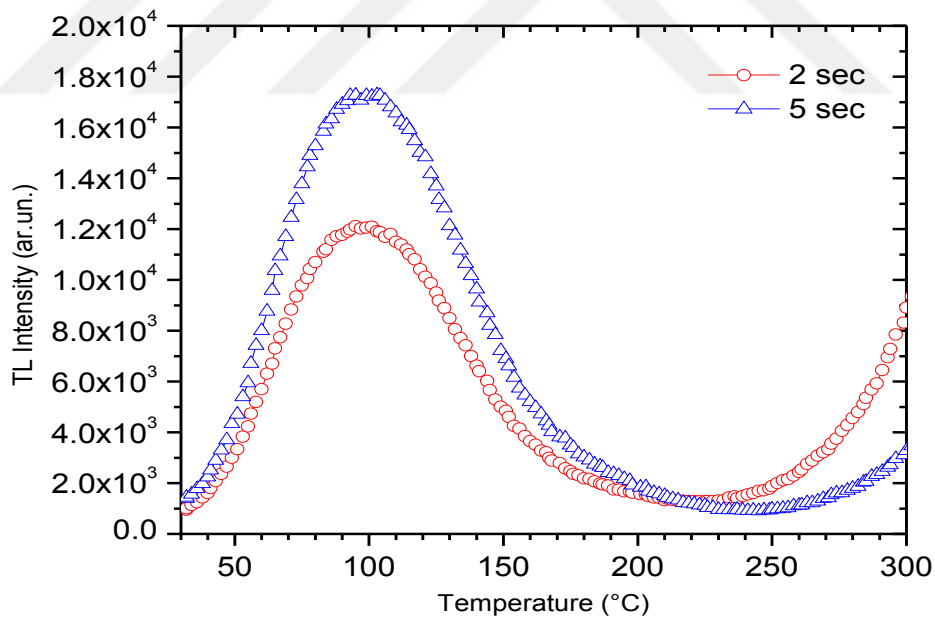
Figure 5.7 Glow curve of Ba_2SiO_4:Dy^{3+} measured after different exposure dose levels (36, 72, and 144) Gy with($\beta = 1°C/s$).

Figure 5.8 Glow curve of Ba_2SiO_4:Dy^{3+} measured after different exposure dose levels (288, 576, and 1152) Gy with ($\beta = 1°C/s$).
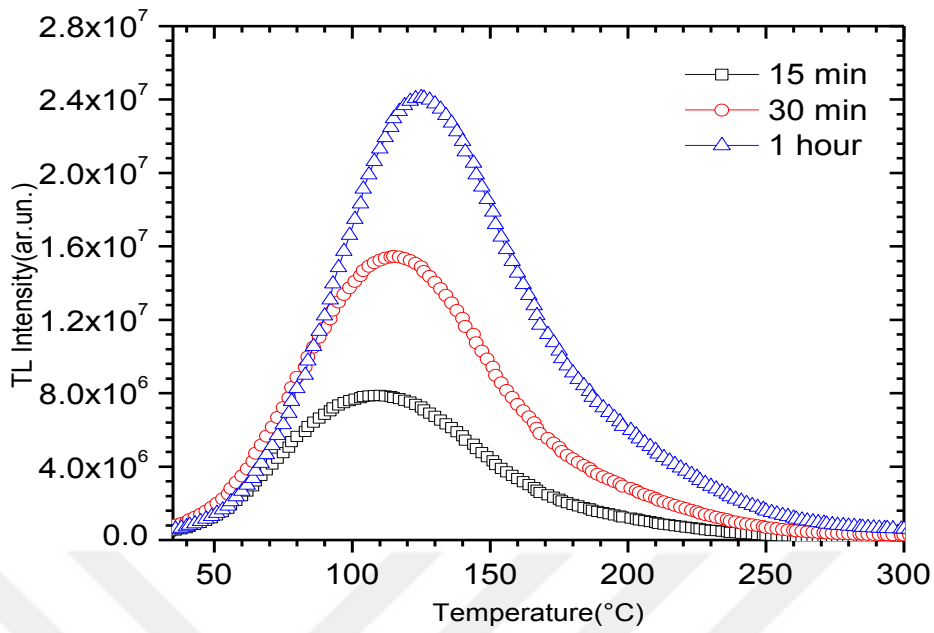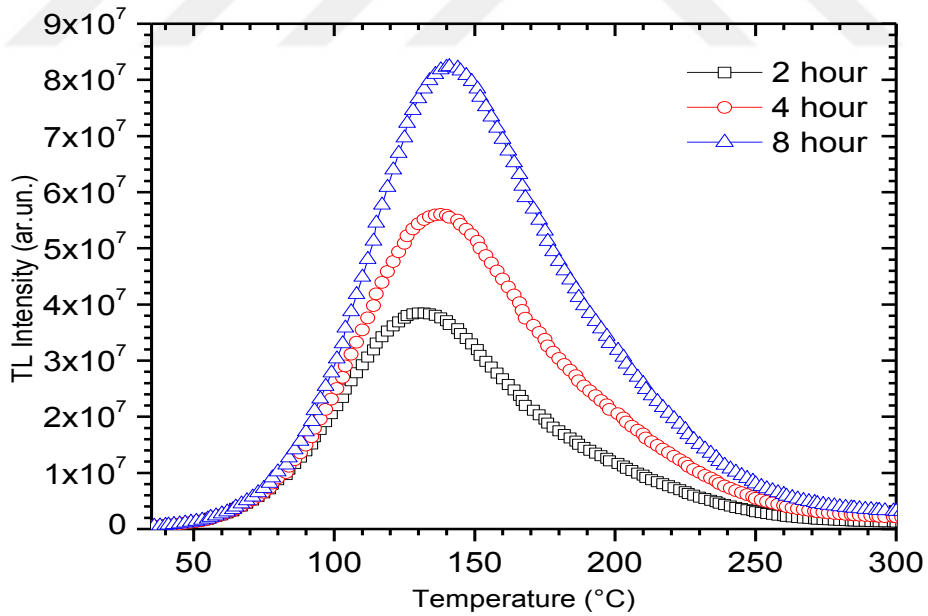
In this current study, the peak height technique was used to realize the impact of linear heating rate between 1 to 5 °C on the structure of the glow curve of Ba_2SiO_4. A sample was with β-ray irradiated by using (36 Gy) ^{90}Sr-^{90}Y irradiation source and the glow curve with the various linear heating rate from 1 to 5°C was obtained shown in Figure 5.9. From this figure, it can understand that by increasing heating rate the peak temperature of glow peak in the Ba_2SiO_4 doped $D_y{}^{+3}$ glow curve was shifted to higher temperature side as expected in theory. It can be seen that with increasing the heating rate the shifting rate of the glow curve decreases and the influence of the heating rate on the glow peaks intensity is roughly equivalent and it more accessible as the heating rate increases.

To explain the decrease in luminescence efficiency, which was continuously observed in TL practice, expression $(\eta = (1 + Cexp(-W/kT)) - 1)$ is proposed, it is known that there is a rivalry between the increase in the probability of a non-radiate with the radiate transition. The luminescence efficiency can be essentially written in the form of $(\eta = P_r/(P_r + P_{nr}))$, where P_r and P_{nr} are the probability of radiated and non-radiated transition, P_r is independent of temperature, but P_{nr} it depends.

Here it is declared that the temperature of the glow curve has shifted to a higher temperature as the heating rate increases, which is why the contribution of non-radiative transition is increased. As a result, it was found that the thermal quenching was higher for the glow peaks present at higher temperatures than the glow peaks present at low temperature in any TLD material. In addition, because at elevated temperature the non-radiated transition probability increases, the observed influence is also assigned on the impact of heating rate on the motion of released charge carriers while reading of TL.

Another important method which is also used for determining the trapping parameter is VHR method. This method was used for the heating rate from 1 to 5°C, as expected the shifting on the position of the temperature (T_m) has happened at the point of intensity (I_m) shown in Figure 5.9, for aim of calculating the activation energy the plot between $\ln(T_m{}^2/\beta)$ against $(1/T_m)$ is drawn in Figure 5.10 then after finding slope easily by multiplying by the Boltzmann constant (k) can be find $E_a = 0.495eV$ shown in Table 5.1.
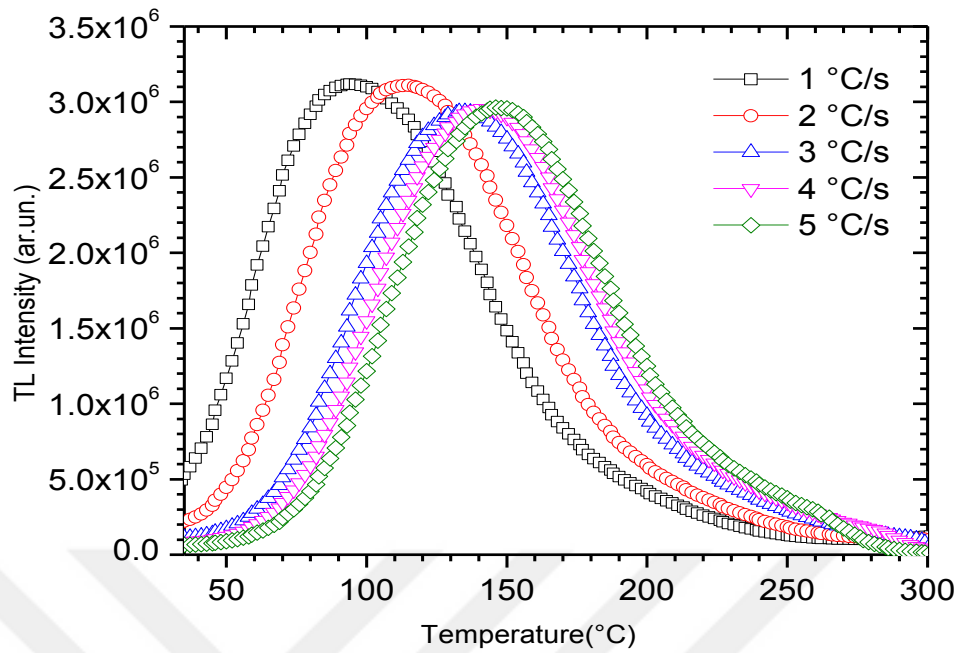
Figure 5.9 Glow curves of $Ba_2SiO_4{:}Dy^{3+}$ measured at the different heating rate for (1, 2, 3, 4, and 5) ℃/s after β irradiation of 36Gy.
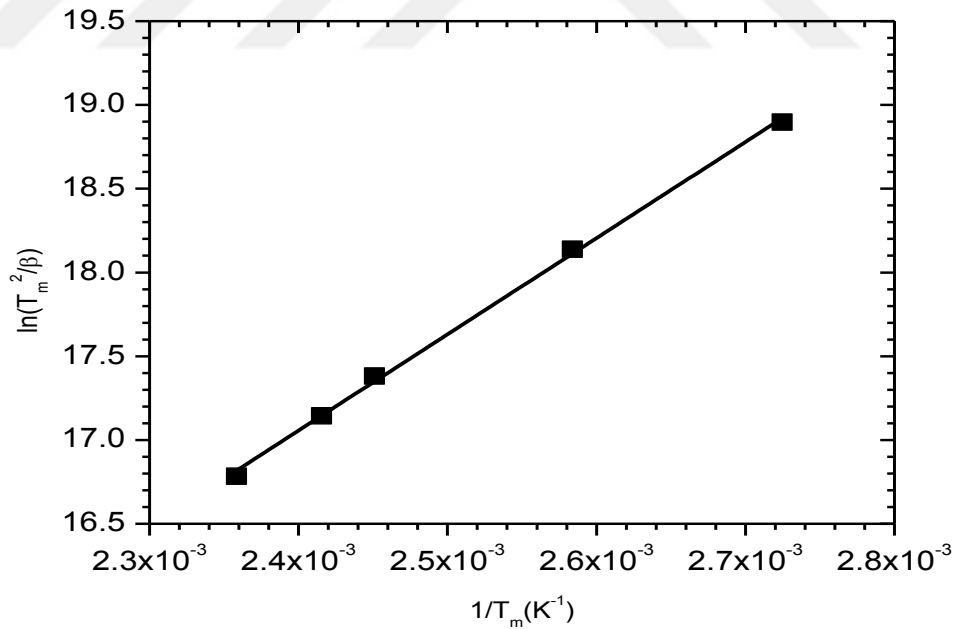
Figure 5.10 Plot of $\ln(T_m^2/\beta)$ versus $1/T_m$ for $Ba_2SiO_4{:}Dy^{3+}$ at heating rate (1, 2, 3, 4, and 5)℃/s.

Since it is very important to know the temperature of the sample accurately for TL measurement, the temperature of the heating strip, not one of the samples, was

measured during the experiment. This difference between the heating element and the sample is known as the temperature lag.

On the other hand, the temperature difference in the sample is known as the temperature gradient, [47, 50] Temperature difference showed a significant impact on TL glow curve and the evaluation of the trapping parameter that can be observed this effect in Figure 5.9. Kits and Tuyn [48, 50] for correcting this temperature lag and temperature gradient problem suggested an approximation method with the TL measure only and it's based on the equation of $T_m^j = T_m^i - C\ln(\frac{\beta_i}{\beta_j})$.

Where β_j and β_i are heating and $\beta_i < \beta_j$, T_m^j and T_m^i are maximum temperature for a given heating rate. C is constant that found at a very slow temperature which TLA neglected.

Another important subject in the application of geological dating, archaeological, environmental and personal dosimeters, and also in dosimeters studies is the stability of signals stored at room temperature. The TL signal stored at ambient room temperature decreases markedly during storage, will result from incompatibility in the result of emitted light and the exposure dose. A time-dependent decrease or loss of radiation-induced signals in a sample can lead to fading.

Fading is a process that is an unintended loss of potential information that response occurs. The fading process has many causes, but thermal energy is the main thing. In thermal fading, as it's clear due to the high probability transition the fade faster for the trap that represents lower capture energy than the higher energy, due to this reason in dose evaluation large errors may generating.

In this experiment 20 mg of the sample $(Ba_2SiO_4:D_y^{+3})$ by 36 Gy was irradiated and to avoid the effect of thermal fading and another external effect the sample after irradiation at room temperature about 27°C and in a dry and dark environment was kept for a period of one week shown in Figure 5.11.

As a display in this TL glow curves as the delay time increased, the intensity of the TL peak at 146°C gradually decreased, corresponding to the continuous release of trapped

carriers in shallow traps. Thus, it concludes that at the room temperature shallow trap in the LLP process it involved.

Moreover, Figure 5.11 also show that maximum peak was located at temperature 146 °C and shifted towards 185 °C after 168 hour due to the shallow traps. This result shows that the depth of the trap is dynamic during the decay process. Therefore, the depth distribution of the trap can be continuous. In addition, this shifting in T_m indicates that the $Ba_2SiO_4:D_y^{+3}$ trapping system is more complex following the first-order kinetics from the Gaussian trap distribution.

Additionally, it reiterates that the re-trapping influence can't be ignored in the late stage of decay. Lastly, it can be seen that from the Figure 5.12 and at the end of the planned storage times the normalized TL area of $Ba_2SiO_4:D_y^{+3}$ reduced 60% of its original value.
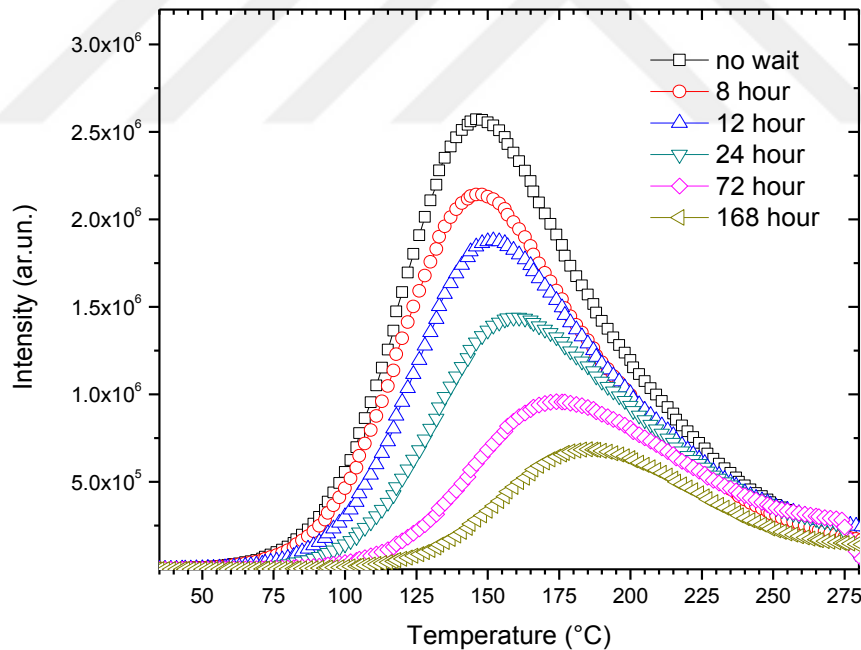

Figure 5.11 A set of TL glow curve for $Ba_2SiO_4:Dy^{3+}$ irradiated by 36Gy and at the various period time of (8, 12, 24, 72, and 168) hour for 1°C/s read out.
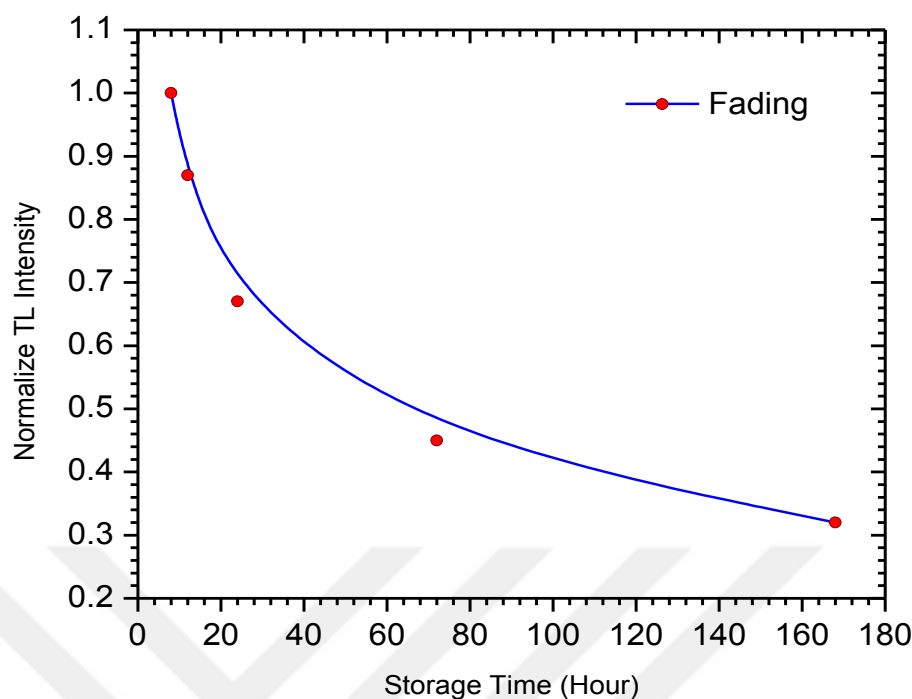
Figure 5.12 Normalized TL intensity for $Ba_2SiO_4{:}Dy^{3+}$ after various storage time (8, 12, 24, 72, and 168) hours at room temperature with 36Gy and heating rate 1℃/s.

Also in this study, instead of deriving the values of the parameters E, S, and b by using a simple formula, the computerized curve fitting method was used for several occasions and clearly succeeded. The procedure is to establish the approximate positions of the most prominent peaks in the glow-curve and to estimate initial values of E, s, and b by using one of the analytical methods discussed so far. A theoretical curve is then computed using the general-order equation for b ≠ 1, or the first-order equation for b=1.

The computed curve is then compared with the actual experimental curve and a Root Mean Square (RMS) deviation between the two is calculated. The procedure continues by sequentially changing the E, s, and b values until a minimum value of the RMS deviation is obtained. This method has the advantage over experimental methods in that they can be used in largely overlapping-peak glow curves without resorting to heat treatment [51]. The program was developed at the Reactor Institute at Delft, Netherlands [52]. This program can simultaneously deconvolute up to nine glow peaks from the glow curve. The computer program used two different models.

Since in the first model it is purified in Chapter 3, the glow curve is approximated from the first-order kinetics TL by expression (3.32), and in the second model, the luminescence curve is approximated by the general-order kinetics TL using the expression (3.33). Summation of the total peaks and the background contribution can lead to the formula of the composite glow curve, as shown in equation (3.34).

Starting from Eq. (3.34), it was judged whether the fitting result was good using the least squares minimization procedure and FOM (Figure of Merit) i.e.

$$FOM = \sum_{i=1}^{n} \frac{\left| N_i(T) - I(T) \right|}{A} = \sum_{i=1}^{n} \frac{\left| \Delta N_i \right|}{A}$$

Where Ni (T) is the (i-th) experimental points (total n= 200 data points), I (T) is the (i-th) fitted points, and A is the integrated area of the fitted glow curve.

Many experiences [41-42], it can be said that if the values of the FOM are between 0.0% and 2.5% the fit is good, 2.5 % and 3.5% the fit is fair, and > 3.5% it is a bad fit. To have a graphic representation of the agreement between the experimental and fitted glow curves, the computer program also plots the function,

$$X(T) = \frac{N_i(T) - I_i(T)}{\sqrt{I_i(T)}}$$

Which is a normal variable with an expected value 0 and $\sigma = 1$ where $\sigma^2(T) = I_i(T)$.

The computerized glow curve deconvolution (CGCD) method has become a very popular way to obtain the kinetic parameters from the glow curves of TL materials. Therefore, the kinetic parameters such as number of glow peaks, activation energies (E_a) and kinetic order (b) for the dosimetric peaks of Dy doped Ba_2SiO_4 were obtained by CGCD method (Fig 5.10) and given in Table 5.1.

In this study, the following general order kinetic analytical equation was used by the approximation for b≈2.

$$I(T) = I_m \cdot b^{b/b-1} \cdot \exp\left(\frac{E}{kT} \cdot \frac{T - T_m}{T_m}\right)$$

$$\cdot \left[(b-1) \cdot (1 - \Delta) \cdot \frac{T^2}{T_m^2} \cdot \exp\left(\frac{E}{kT} \cdot \frac{T - T_m}{T_m}\right) + Z_m\right]^{-b/b-1}$$

49

Where;

$$\Delta = \frac{2kT}{E} \quad , \qquad \Delta_m = \frac{2kT_m}{E} \quad , \quad Z_m = 1 + (b - 1) \cdot \Delta_m$$
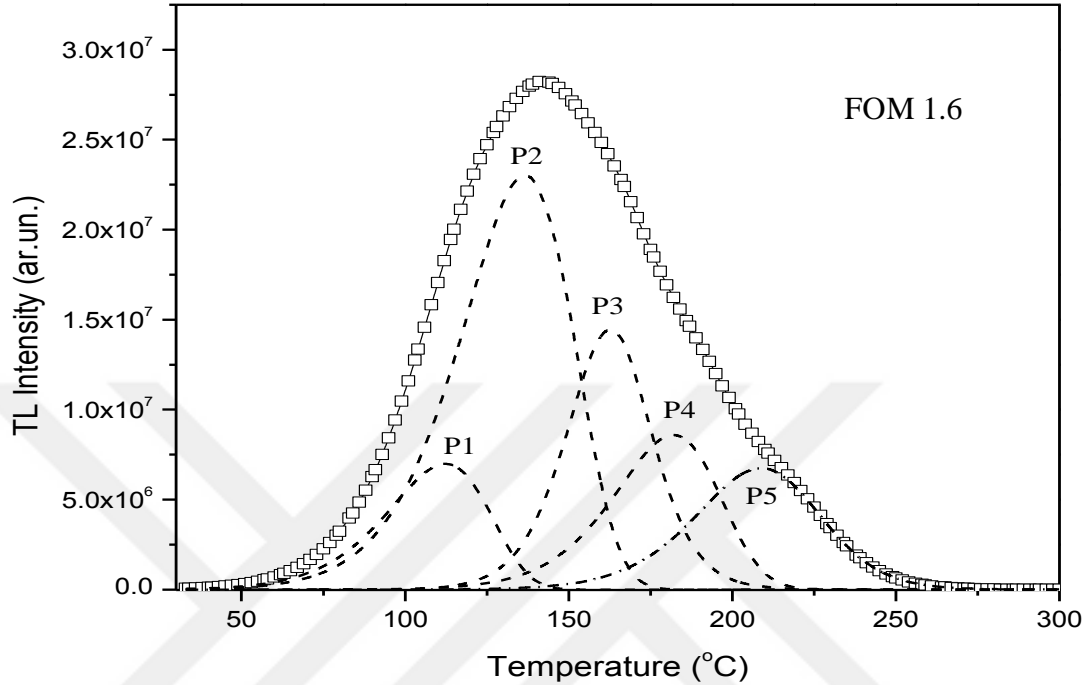
Figure 5.13 Computerized glow curve deconvolution results for Ba_2SiO_4 measured after 144 Gy irradiation by beta ray at room temperature with $(\beta = 1 \ ^{o}C.s^{-1})$ (FOM: 1,6).

The number of glow peaks is not a free fitting parameter during the deconvolution of the measured glow curve into individual components in the CGCD programs. If the number of peaks is not known, it can be found by fitting the glow curve several times with a different number of components up to obtaining a best-fit result.

In this study, after many tries with different number of glow peaks, it was observed that the glow curve structures of Ba_2SiO_4 is well described by a linear combination of at least five glow peaks. In this case, a reasonably good fit was always obtained. Some of the analyzed and deconvoluted glow curves of both dosimeters after mixed β-irradiations are shown in Figures 5.13. The obtained results of E_a, s, and b by using the CGCD methods are shown in Table 5.1.

Table 5.1 The trapping parameter value of $Ba_2SiO_4:Dy^{3+}$.

	Chen P.S.			Mazumdar P.S.			H.Rate	CGCD For P2
	E_τ	E_δ	E_ω	1/2 ratio	2/3 ratio	4/5 ratio		
E_a (eV)	0.47	0.52	0.50	0.47	0.46	0.466	0.495	0.552
b	2	2	2	2	1.90	1.85	2	2
lns (s^{-1})	14.9	14.9	14.9	13.91	13.91	13.91	14.79	14.55

CHAPTER 6

CONCLUSION

The foremost goal of our study was to find thermoluminescence kinetic parameters of Ba_2SiO_4 doped with Dy^{3+} after ^{90}Sr-^{90}Y beta irradiation, which is also finding these kinetic parameters that namely the order of kinetics (b), activation energy (E_a) and the frequency factor (s) it is very helpful to understand the thermoluminescence properties of $Ba_2SiO_4:Dy^{3+}$. The different experimental techniques were used for determining these parameters which were associated with the thermoluminescence of the glow peak the methods are an additive dose (AD), peak shape (PS), variable heating rate (VHR) and computerized glow deconvolution (CGCD) methods.

In this study, we used the Additive Dose experiment (AD) to examine the dose-dependent characteristics of the glow curve of barium silicate ($Ba_2SiO_4:Dy^{3+}$). Dose dependence was investigated by irradiating the sample at different dosage levels between 2sec $\approx$ 0.08Gy to 8-hour $\approx$ 1152Gy in the temperature range from room temperature to 400 °C at a linear heating rate of 1 °C/s and the result was specified that there is overlap of at least two glow peaks. Experimental tests showed that there was no major shift in the site of peak temperature and there was a slight change in temperature and nearly constant with increasing dose level as its shown in Figure 5.4 to 5.8. The value of kinetic parameters of order of kinetics (b), Activation Energy (E_a) and the frequency factor (s) was founded by methods of an Additive Dose (AD), Peak Shape (PS), Variable Heating Rate (VHR) and Computerized Glow Curve Deconvolution (CGCD) methods. As a result, Chen's peak shape methods give values kinetic parameters b=2, E_a=0.49ev, $\ln(s)$=14.9. Although Mazumdar peak shape method was used and the result are b=1.9, E_a=0.465ev, $\ln(s)$=13.91. As can be seen in Figure 5.9 by increasing heating rate the peak temperature in the Ba_2SiO_4 doped D_y^{+3} glow curve was shifted to higher temperature side and with increasing the heating rate the shifting rate of the glow curve decreases and the influence of the heating rate on the glow peaks intensity is roughly equivalent and it more accessible as the heating

rate increases. Although due to HR method kinetic parameters were founded and results are b=2, E_a= 0.495 eV, ln(s)= 14.79.

As mentioned before, this study has been supported by CGCD program with analyzing the measured glow curves. It is a very popular method to evaluate the absorbed dose and trapping parameters of glow peaks from the glow curves. Because during the curve fitting procedure whole curve points are utilized in the analysis, rather than just a few points on the glow curve, Figure 5.13 shows the results of CGCD fitting of irradiated (Ba_2SiO_4: Dy) by a β-ray with 144Gy on the assumption of two peaks with summarizes values of kinetic parameter values for each of the peaks, and TL glow curve analyzer software with the figure of Merit (FOM) values 1.6%. The values evaluated with CGCD method for P2 and parameters are equal b=2, E_a=0.552 eV, ln(s)=14.55. All these values can be seen in detail in Table 5.1.

In the experiment of the storage time the sample $Ba_2SiO_4:Dy^{3+}$ by 36 Gy was irradiated and to avoid the effect of thermal fading and another external effect the sample after irradiation at room temperature 27 ℃ and in a dry and dark environment was kept for a different storage time from 8 hours to one week shown in Figure 5.11 and 5.12. It can be seen that from the Figure 5.12 and at the end of the planned storage times the normalized TL area of $Ba_2SiO_4:Dy^{3+}$ reduced 60% of its original value. To solve this problem, we recommend adding multiple co-dopants to the host lattice. Therefore, our measurements provide some additional information on the properties of $Ba_2SiO_4:Dy^{3+}$.

REFERENCES

[1] Chen, R. McKeever. S. (1997). Theory of Thermoluminescence and Related. *World Scientific Publishing Co. Pte. Ltd., Singapore.*

[2] McKeever, S.W.S. (1985). Thermoluminescence of Solids. Pub. *Cambridge University Press.* 374.

[3] Murthy, K. V. R. (2000). Luminescence Applications Few Basics, Pub. *Luminescence Society of India,* **3**, 302-315.

[4] Aitken, M. J. (1985). Thermoluminescence dating. Pub. *Academic Press*, 331-351.

[5] Randall, J. T., and Wilkins, M. H. F. (1945). Phosphorescence and electron traps I: The study of trap distributions. *Proceedings of Royal Society A* **184**, 366-389.

[6] Pradhan, A.S. (1981). Radiation Protection Dosimetry, **1**, 153.

[7] Pekpak, E., Gülhan, O., Aysen, Y. (2009). Thermoluminescent characteristics of lithium tetraborate, in: Proceedings of the *IV International Boron Symposium.*

[8] Furetta, C. (2010). *Handbook of thermoluminescence*. World Scientific.

[9] Mahesh, K., Weng, P. S., and Furetta, C. (1989). Thermoluminescence in Solids and its Applications. Ashford, Kent, England: Nuclear Technology Publishing.

[10] Schipper, W.J., Blasse, G., and Leblans, P. (1994). Chemistry of Materials, **6**, 1784 − 1789.

[11] Jia, D., & Yen, W. M. (2003). Enhanced $V_K{}^{3+}$ center afterglow in $MgAl_2O_4$ by doping with Ce^{3+}. *Journal of luminescence*, **101**, 115-121.

[12] McKeever, S. W. S. (1985). Thermoluminescence of Solids, Cambridge, Univ. *Press Cambridge*, **32**.

[13] Harvey, E. (2005). A History of Luminescence: From the Earliest Times Until 1900. USA: Dover Phoenix Editions.

[14] Newton Harvey, E. (1957). A History of Luminescence: From the Earliest Times until 1900, Philadelphia: The American Philosophical Society, Independence Square.

[15]Chen, R., Yang, X.H. & McKeever, S.W.S, (1988) Strongly Superlinear Dose Dependence of Thermoluminescence in Synthetic Quartz, *J. Phys. D: Appl. Phys*., **21**, 1312.

[16] McKeever, SWS., Moskovitch, M., and Townsend, P.D. (1995). Thermoluminescence Dosimetry Materials: Properties and Uses. Ashford, England: Nuclear Technology Publishing.

[17] Yamaga, M., Masui, Y., Sakuta, S., Kodama, N., & Kaminaga, K. (2005). Radiative and nonradiative decay processes responsible for long-lasting phosphorescence of Eu^{2+}-doped barium silicates, Pub. *Physical Review B*, **71**, 205102.

[18] Yao, S., Li, Y., Xue, L., & Yan, Y. (2010). Photoluminescence properties of $Ba_2ZnSi_2O_7$: Eu^{2+}, Re^{3+} (Re= Dy, Nd) long-lasting phosphors prepared by the combustion-assisted synthesis method, pub. *Journal of Alloys and Compounds*, **490**, 200-203.

[19] Wang, M., Zhang, X., Hao, Z., Ren, X., Luo, Y., Wang, X., & Zhang, J. (2010). Enhanced phosphorescence in N contained Ba_2SiO_4: Eu^{2+} for X-ray and cathode ray tubes, Pub. *Optical Materials*, **32**, 1042-1045.

[20] Sakamoto, T., Uematsu, K., Ishigaki, T., Toda, K., & Sato, M. (2011). Development of gas-solid phase hybrid synthesis method of single crystal Ba_2SiO_4: Eu^{2+}, pub. *Key Engineering Materials* Trans Tech Publications, **485**, 325-328.

[21] Streit, H. C., Kramer, J., Suta, M., & Wickleder, C. (2013). Red, green, and blue photoluminescence of Ba_2SiO_4: M (M= Eu^{3+}, Eu^{2+}, Sr^{2+}) nano-phosphors, pub. *Materials*, **6**, 3079-3093.

[22] Choi, J. I., Anc, M., Piquette, A., Hannah, M. E., Mishra, K. C., Talbot, J. B., & McKittrick, J. (2014). Electrophoretic deposition of nano-and micron-sized Ba_2SiO_4: Eu^{2+} phosphor particles, pub. *Journal of The Electrochemical Society*, **161**, 111-117.

[23] Wang, P., Xu, X., Zhou, D., Yu, X., & Qiu, J. (2015). Sunlight activated long-lasting luminescence from $Ba_5Si_8O_{21}$: Eu^{2+}, Dy^{3+} phosphor, pub. *Inorganic chemistry*, **54**, 1690-1697.

[24] Zhang, B., Zhang, J. W., Zhong, H., Hao, L. Y., Xu, X., Agathopoulos, S., & Yin, L. J. (2017). Enhancement of the stability of green-emitting Ba_2SiO_4: Eu^{2+} phosphor by hydrophobic modification, pub. *Materials Research Bulletin*, **92**, 46-51.

[25] Bos, A.J.J. & Dielhof, J.B. (1991). The analysis of thermoluminescent glow curves in CaF_2: Tm (TLD-300). *Radiation Protection Dosimetry*, **36**, 231-239.

[26] Venderschueren, J., & In, J. C. (1979). P. Braunlich, Editor, pub. *Thermally stimulated relaxation in solids*.

[27] McKeever, S. W. S. (1985). Thermoluminescence of Solids, Cambridge, Univ. *Press Cambridge*, *32*.

[28] Kitis, G., Gomez-Ros, J.M., and Tuyn, J.W.N. (1998). Thermoluminescence glow curve deconvolution functions for first, second and general orders of kinetics, *Journal of Physics D:Applied Physics*, **31**, 2636-2641.

[29] Boss, A.J.J. (2007). Theory of thermoluminescence, *Radiation measurements*, **41**, 45-56.

[30] Hoogenboom, J.R., de Vries, W., Dielhof, J.B., Bos, A.J.J., (1988). Computerized analysis of glow curves from thermally activated processes, *Journal of Applied Physics*. **64**, 3193–3200.

[31] Garlick, G. F. J., and Gibson. A. F. (1948). The electron trap mechanism of luminescence in sulfide and silicate phosphors, *Proceedings of Physics Society,* **60**, 574.

[32] Bos, A.J.J., and Dielhof, J.B. (1991). The analysis of thermoluminescent glow curves in CaF_2: Tm(TLD-300), *Radiation Protection Dosimetry*. **37**, 231–239.

[33] May, C.E., and Partridge, J.A. (1964). Thermoluminescence kinetics of alpha irradiated alkali halides, *Journal of Chemical Physics*, **40**, 1401-1415.

[34] Gómez Ros, J.M., Kitis, G., (2002). Computerised glow curve deconvolution using general and mixed order kinetics, *Radiation Protection Dosimetry*. **101** (1–4), 47–52.

[35] Azorin, J. (1986). Determination of thermoluminescence parameters from glow curves-I. A review, *Nuclear Tracks & Radiation Measurements*, **11**, 159-166.

[36] Chen, R., and Winer, A.A. (1970). Effects of various heating rates on glow curves, *Journal of Applied Physics*, **41**, 5227-5232.

[37] Chen, R., McKeever, S.W.S. (1994). Characterization of nonlinearities in the dose dependence of thermoluminescence. Radiation Measurements, **23**, 667- 673.

[38] Chen, R. (1969). On the Calculation of Activation Energies and Frequency Factors from Glow Curve, *Journal of Applied Physics*, **40**, 570.

[39] Halperin, A., and Braner, A.A. (1960). Evaluation of thermal activation energies from glow curves, *Physical Review Letters*, **117**, 408-415.

[40] Gartia, R. K., Singh, S. J., & Mazumdar, P. S. (1989). Determination of the Activation Energy of Thermally Stimulated Luminescence Peaks Obeying General-Order Kinetics. *physical status solidi (a)*, **114**, 407-411.

[41] Hsu, P.C. & Wang, T.K. (1986). On the annealing procedure of CaF_2:Dy. Radiation Protection Dosimetry, **16**, 253-256.

[42] Mahesh K., Weng P.S. & Furetta C. (1989). Thermoluminescence in Solids and Applications. Nuclear Technology Publishing; Ashford, Kent TN25 4NW England ISBN 1870965000.

[43] McKeever, S.W.S., Moscovitch, M. & Townsend, P.D. (1995). Thermoluminescence Dosimetry Materials: Properties and Uses, Nuclear Technology Publishing, Ashford, Kent TN23 1YW England.

[44] McKeever, S.W.S., (1983). *Thermoluminescence of solids*. Oklahoma State University Press.

[45] Piters, T.M. & Bos, A.J.J. (1993). Thermoluminescence Emission Spectra of LiF (TLD-100) after different Thermal Treatments. *Journal of Physics D:Applied Physics*, **47**, 91-94.

[46] Kitis, G., and Pagonis, V. (2007). Peak shape methods for general order thermoluminescence glow-peaks: a Reappraisal, *Nuclear Instrumentation and Methods B.*, **262,** 313-322.

[47] Furetta, C., Kitis, G., Kuo, J. H., Vismara, L., & Weng, P. S. (1997). Impact of non-ideal heat transfer on the determination of thermoluminescent kinetics parameters. *Journal of luminescence*, **75**, 341-351.

[48] Kitis, G., & Tuyn, J. W. N. (1998). A simple method to correct for the temperature lag in TL glow-curve measurements. *Journal of Physics D: Applied Physics*, **31**, 2065.

[49] Grossweiner, L.I. (1953). A note on the Analysis of First-Order Glow curves. *Journal of Applied Physics*, **24**, 1306-1308.

[50] Kitis, G., Kiyak, N. G., & Polymeris, G. S. (2015). Temperature lags of luminescence measurements in a commercial luminescence reader. *Nuclear Instruments and Methods in Physics Research Section B: Beam Interactions with Materials and Atoms*, **359**, 60-63.

[51] Horowitz, Y.S., and Yossian, D. (1995). Computerized Glow Curve Deconvolution: Application to Thermoluminescence Dosimetry. *Radiation Protection Dosim*etry, **60,** 5-12.

[52] Bos, A.J.J., Piters, J. M., Gomez Ros, J. M., and Delgado, A. (1993). GLACANIN, and Intercomparison of Glow Curve Analysis Computer Programs: IRI-CIEMAT Report 131-93-005 IRI Delft.

[53] Dorenbos, P. (2005). Mechanism of persistent luminescence in $Sr_2MgSi_2O_7$: Eu^{2+}; Dy^{3+}. *physical status solidi (b), 242*.

[54] Clabau, F., Rocquefelte, X., Jobic, S., Deniard, P., Whangbo, M. H., Garcia, A., & Le Mercier, T. (2005). Mechanism of phosphorescence appropriate for the long-lasting phosphors Eu^{2+}-doped $SrAl_2O_4$ with co-dopants Dy^{3+} and B^{3+}. *Chemistry of Materials*, **17**, 3904-3912.

[55] Yamazaki, K., Nakabayashi, H., Kotera, Y., & Ueno, A. (1986). Fluorescence of Eu^{2+}-Activated Binary Alkaline Earth Silicate. *Journal of The Electrochemical Society*, **133**, 657-660.

[56] Barry, T. L. (1968). Equilibria and Eu^{2+} Luminescence of Subsolidus Phases Bounded by $Ba_3MgSi_2O_8$, $Sr_3MgSi_2O_8$, and $Ca_3MgSi_2O_8$. *Journal of The Electrochemical Society*, **115**, 733-738.

[57] Lee, J. H., & Kim, Y. J. (2008). Photoluminescent properties of Sr_2SiO_4: Eu^{2+} phosphors prepared by solid-state reaction method. *Materials Science and Engineering: B*, **146**, 99-102.

[58] Poort, S. H. M., Reijnhoudt, H. M., Van der Kuip, H. O. T., & Blasse, G. (1996). Luminescence of Eu^{2+} in silicate host lattices with alkaline earth ions in a row. *Journal of alloys and compounds*, **241**, 75-81.

[59] Barry, T. L. (1968). Fluorescence of Eu^{2+}-Activated Phases in Binary Alkaline-Earth Orthosilicate Systems. *Journal of the Electrochemical Society*, **115**, 1181-1184.

[60] Gupta, K. K., Kadam, R. M., Dhoble, N. S., Lochab, S. P., Singh, V., & Dhoble, S. J. (2016). Photoluminescence, thermoluminescence and evaluation of some parameters of Dy^{3+} activated $Sr_5(PO_4)_3F$ phosphor synthesized by sol-gel method. *Journal of Alloys and Compounds*, **688**, 982-993.

[61] Bos A J J, Piters J M, Gomez Ros J M and Delgado A 1993 (GLOCANIN and Intercomparision of Glow Curve Analysis Computer Programs) IRI-CIEMAT Report 131-93-005 IRI Delft.

[62] Horowitz Y S, Yossian D 1995 Application to Thermoluminescence Dosimetry Radiat. Prot. Dosim **60,** 1-114.

[63] Afouxenidis D, Polymeris G S, Tsirliganis N C and Kitis G 2012 Radiation Protection Dosimetry **149,** 363-370.